

NASA TECHNICAL
MEMORANDUM



NASA TM X-1942

NASA TM X-1942

CASE FILE
COPY

STATIC STABILITY, CONTROL,
AND FIN LOAD CHARACTERISTICS OF
A MODEL OF AN APACHE VEHICLE WITH
A COAST-PHASE-CONTROL PACKAGE

by William J. Monta

Langley Research Center

Langley Station, Hampton, Va.

NATIONAL AERONAUTICS AND SPACE ADMINISTRATION • WASHINGTON, D. C. • FEBRUARY 1970

1. Report No. NASA TM X-1942	2. Government Accession No.	3. Recipient's Catalog No.	
4. Title and Subtitle STATIC STABILITY, CONTROL, AND FIN LOAD CHARACTERISTICS OF A MODEL OF AN APACHE VEHICLE WITH A COAST-PHASE-CONTROL PACKAGE		5. Report Date February 1970	
7. Author(s) William J. Monta		6. Performing Organization Code	
9. Performing Organization Name and Address NASA Langley Research Center Hampton, Va. 23365		8. Performing Organization Report No. L-6835	
12. Sponsoring Agency Name and Address National Aeronautics and Space Administration Washington, D.C. 20546		10. Work Unit No. 126-63-11-15-23	
		11. Contract or Grant No.	
		13. Type of Report and Period Covered Technical Memorandum	
14. Sponsoring Agency Code			
15. Supplementary Notes			
16. Abstract An investigation has been conducted in the Langley Unitary Plan wind tunnel at Mach numbers from 1.60 to 2.87 to determine the aerodynamic characteristics of a model of an Apache second-stage vehicle equipped with a coast-phase-control system section having interdigitated movable cruciform fins. The results indicated a pitchup tendency that becomes more pronounced with increasing Mach number. The fins were effective in producing pitch and roll control throughout the test range of angle of attack and Mach number. At the higher angles of attack, roll-control deflection induced some adverse yawing moments.			
17. Key Words Suggested by Author(s) Aerodynamic characteristics Aerodynamic loads Static stability and control		18. Distribution Statement Unclassified – Unlimited	
19. Security Classif. (of this report) Unclassified	20. Security Classif. (of this page) Unclassified	21. No. of Pages 33	22. Price* \$3.00

*For sale by the Clearinghouse for Federal Scientific and Technical Information
Springfield, Virginia 22151

STATIC STABILITY, CONTROL, AND FIN LOAD CHARACTERISTICS OF
A MODEL OF AN APACHE VEHICLE WITH
A COAST-PHASE-CONTROL PACKAGE

By William J. Monta
Langley Research Center

SUMMARY

An investigation has been conducted in the Langley Unitary Plan wind tunnel at Mach numbers from 1.60 to 2.87 to determine the aerodynamic characteristics of a model of an Apache second-stage vehicle equipped with a coast-phase-control system section having interdigitated movable cruciform fins.

The results indicated a pitchup tendency that becomes more pronounced with increasing Mach number. The fins were effective in producing pitch and roll control throughout the test range of angle of attack and Mach number. At the higher angles of attack, roll-control deflection induced some adverse yawing moments.

INTRODUCTION

A rocket vehicle is required for use as a simulated target to check radar acquisition systems. One proposed vehicle consists of a Nike-Ajax first-stage booster and an Apache second stage. In an effort to achieve a minimum impact dispersion, the vehicle was provided with a coast-phase-control system consisting of a cylindrical section with movable cruciform fins placed between the first and second stages. The control fins are interdigitated with respect to the fixed Apache fins. Flight tests of the vehicle revealed unsatisfactory characteristics and necessitated a change in the design of the control fins. It was deemed desirable to obtain a more detailed examination of the stability and control characteristics of the vehicle that would include a determination of the load characteristics of the control fins. Accordingly, the Langley Research Center has undertaken a wind-tunnel investigation to determine these characteristics on a 0.30-scale model of the second-stage Apache vehicle equipped with the coast-phase-control system.

Tests were performed in the Langley Unitary Plan wind tunnel at Mach numbers from 1.60 to 2.87 at a constant unit Reynolds number near 2.0×10^6 per foot (6.6×10^6 per meter). The tests were conducted over an angle-of-attack range from about -90° to 90° . The 0.30-scale model was too long to provide data free of shock reflections below Mach 2; therefore, approximately one-half of the cylindrical section ahead of

the wings was removed to permit testing at Mach 1.6 with a foreshortened model. It was assumed that the loads on the control fins would not be greatly affected by this model change, and that the resulting stability and control data would aid in evaluating the true model characteristics at Mach 1.6.

SYMBOLS

The longitudinal aerodynamic force and moment data are referred to both the stability and body axes systems. The lateral aerodynamic data are referred only to the body axis system. The moment data are referred to a longitudinal position 11.4 inches (28.96 cm) from the model base for both the basic model and the foreshortened model. Symbols used are defined as follows:

$b/2$ exposed fin semispan

\bar{c} fin mean aerodynamic chord

c_r exposed fin root chord

c_t tip chord

C_A axial-force coefficient, $\frac{\text{Axial force}}{qS_{\text{ref}}}$

$C_{A,b}$ base axial-force coefficient, $\frac{\text{Base axial force}}{qS_{\text{ref}}}$

C_B fin-panel bending-moment coefficient, measured about exposed root-chord line, $\frac{\text{Bending moment}}{qS_{\text{fin}} \frac{b}{2}}$

C_D drag coefficient, $\frac{\text{Drag}}{qS_{\text{ref}}}$

$C_{D,b}$ base-force drag coefficient, $\frac{\text{Base drag}}{qS_{\text{ref}}}$

$C_{D,o}$ drag coefficient at zero lift

C_h fin hinge-moment coefficient, measured about hinge line, $\frac{\text{Hinge moment}}{qS_{\text{fin}} \bar{c}}$

C_l	rolling-moment coefficient, $\frac{\text{Rolling moment}}{qS_{\text{ref}}d}$
C_L	lift coefficient, $\frac{\text{Lift coefficient}}{qS_{\text{ref}}}$
$C_{L\alpha}$	lift curve slope, per degree
C_m	pitching-moment coefficient, $\frac{\text{Pitching moment}}{qS_{\text{ref}}d}$
$C_{m\delta}$	pitch control effectiveness, per degree
C_N	normal-force coefficient, $\frac{\text{Normal force}}{qS_{\text{ref}}}$
C_n	yawing-moment coefficient, $\frac{\text{Yawing moment}}{qS_{\text{ref}}d}$
d	reference body diameter
l	body length
M	free-stream Mach number
q	free-stream dynamic pressure
S	area
S_{base}	base cross-sectional area
S_{fin}	fin-panel planform area
S_{ref}	body cross-sectional reference area
x_{ac}	axial distance from model nose tip to aerodynamic center
α	angle of attack
δ	fin deflection angle, deg

Λ sweep angle, deg

Subscripts:

1,2,3,4 fin numbers (see fig. 1)

APPARATUS AND METHODS

Tunnel

Tests were conducted in the low Mach number test section of the Langley Unitary Plan wind tunnel, which is a variable-pressure continuous-flow facility. The test section is approximately 4 feet (1.219 m) square and 7 feet (2.134 m) long. The nozzle leading to the test section is of the asymmetric sliding-block type which permits a continuous variation in Mach number from about 1.5 to 2.9.

Model

The model and fin load instrumentations were furnished by the Physical Science Laboratory of New Mexico State University. Dimensional details of the 0.3-scale model are presented in figure 1 and table I, and a photograph of the model is presented in figure 2. The overall model was 60.00 inches (152.4 cm) long with a maximum forebody diameter of 2.043 inches (5.189 cm). The major features of the model include fixed cruciform wings and aft interdigitated movable control fins. (See table II.) Four antenna housings were also included on the model. A 15-inch (38.1 cm) portion of the cylindrical section between the antenna and the wings was made removable in order to permit shock-reflection-free testing at $M = 1.60$.

Test Conditions and Instrumentation

The test conditions for the investigation were as follows:

Mach number	Stagnation temperature		Stagnation pressure		Unit Reynolds number	
	°F	°K	lb/sq ft abs	kN/m²	1/ft	1/m
1.60	150	339	1141	54.63	2.0×10^6	6.6×10^6
2.00	150	339	1327	63.54	2.0	6.6
2.50	150	339	1698	81.30	2.0	6.6
2.87	150	339	2056	98.44	2.0	6.6

Tests were made through an angle-of-attack range from -90° to 90° . The dewpoint was maintained below -30° F (239° K) in order to assure negligible condensation effects.

Boundary-layer transition strips composed of 1/16-inch (0.16-cm) bands of sand were affixed around the nose 1.2 inches (3.1 cm) from the apex and on all lifting surfaces 0.4 inch (1.0 cm) aft of the leading edge in a streamwise direction. Number 40 sand (0.018 inch (0.05 cm) nominal height) was used on the nose, and number 60 sand (0.011 inch (0.03 cm) nominal height) was used on the other surfaces.

Aerodynamic forces and moments were measured by means of a six-component electrical strain-gage balance housed within the model. The balance, in turn, was rigidly fastened to a sting support and then to the tunnel support system. The fins were instrumented with three-component, electrical strain-gage beams. Model base pressure was measured by means of a single static orifice placed in the balance cavity. All tests were made with the wings in 45° planes, and the control fins in the horizontal and vertical planes. Tests were made with the 45-inch (114 cm) model at $M = 1.60$ and 2.00, and with the 60-inch (152-cm) model at $M = 2.00, 2.50$, and 2.87. The tests at $M = 2.00$ were made with both the 45-inch and 60-inch configurations primarily to obtain a direct comparison of stability levels of the two configuration lengths.

Corrections

Angle of attack was corrected for both tunnel flow angularity and deflection of the sting-balance combination due to aerodynamic loads. The axial-force and drag coefficient data have been adjusted to correspond to free-stream static pressure acting over the model base. Typical base axial-force and base drag coefficients are presented in figure 3.

PRESENTATION OF RESULTS

	Figure
Longitudinal characteristics:	
Effect of pitch control	4
Summary of pitch characteristics	5
Lateral characteristics:	
Effect of roll control deflection	6
Fin load characteristics:	
Effect of pitch control deflection	7

DISCUSSION

Stability and Control

The aerodynamic characteristics in pitch for the test configurations are presented in figure 4 for several pitch-control deflections. (Although these data are presented about both the body and the stability axes systems, only the stability axis data will be discussed.) The variation of lift coefficient with angle of attack is relatively linear, although the pitching-moment variation with lift exhibits a pitchup tendency that becomes more pronounced with increasing Mach number (fig. 4(d), for example). The fins are effective in providing pitch control over the Mach number range, and they produce reasonably linear increments in pitching moment that are essentially constant over the angle-of-attack range. It should be noted that there is a loss in lift coefficient and an increase in drag coefficient accompanying the increase in control deflection.

The summary of several longitudinal parameters presented in figure 5 indicates the expected decrease in $C_{L\alpha}$, $C_{D,0}$, and $C_{m\delta}$ with increase in Mach number. The data also indicate a small forward shift in aerodynamic center with increase in Mach number.

The roll-control effectiveness of the fins is shown in figure 6. The fins are effective in producing roll control throughout the test Mach number range, and the incremental rolling moments generated are relatively linear with control deflection. Variation in angle of attack causes some changes in fin effectiveness, and the effectiveness does decrease slightly with Mach number. A small adverse yawing moment caused by roll control is induced at the higher test angles of attack.

Fin Loads

The variations of normal force, hinge moment, and bending moment with angle of attack for various fin deflection angles are presented in figure 7 for the right-hand fin only. The results for the left-hand fin are essentially identical when allowance is made for the slight difference in fin incidence angles (table II) due to misalignment between the two fins. The data at $M = 2.00$ for the long and short configurations are essentially the same; thus, the $M = 1.6$ fin loads measured on the 45-inch (114 cm) body can be considered to be applicable to the correct model length (60-inch (152 cm)) configuration. The slopes of the normal-force and bending-moment curves decrease with increase in Mach number, as would be expected. The hinge-moment data, on the other hand, increase with increase in Mach number and indicate that the longitudinal center of pressure is moving further aft of the hinge line.

CONCLUDING REMARKS

Tests of a 0.30-scale model of an Apache second-stage vehicle, equipped with a coast-phase-control system section having movable cruciform fins, have been made at Mach numbers from 1.60 to 2.87.

The results indicated a pitchup tendency that becomes more pronounced with increasing Mach number. The fins were effective in producing pitch and roll control throughout the test range of angle of attack and Mach number. At the higher angles of attack, roll-control deflection induced some adverse yawing moments.

Langley Research Center,
National Aeronautics and Space Administration,
Langley Station, Hampton, Va., October 30, 1969.

TABLE I.- GEOMETRIC CHARACTERISTICS

(a) Wings, fins, and antennas

	Wings		Fins		Antennas
Aspect ratio, $2(b/2)^2/S$	1.33		1.49		0.324
b/2, in. (cm)	3.00	(7.62)	1.95	(4.95)	0.30 (0.76)
Λ , leading edge, deg		45		45	45
Λ , trailing edge, deg		0		0	0
\bar{c} , in. (cm)	4.67	(11.85)	2.75	(6.98)	1.85 (4.71)
c_r , in. (cm)	6.00	(15.24)	3.60	(9.14)	2.00 (5.08)
c_t/c_r , taper ratio		0.50		0.46	0.85
S, ft^2 (m^2), per panel	0.0940	(0.00873)	0.0355	(0.00330)	0.00385 (0.000358)

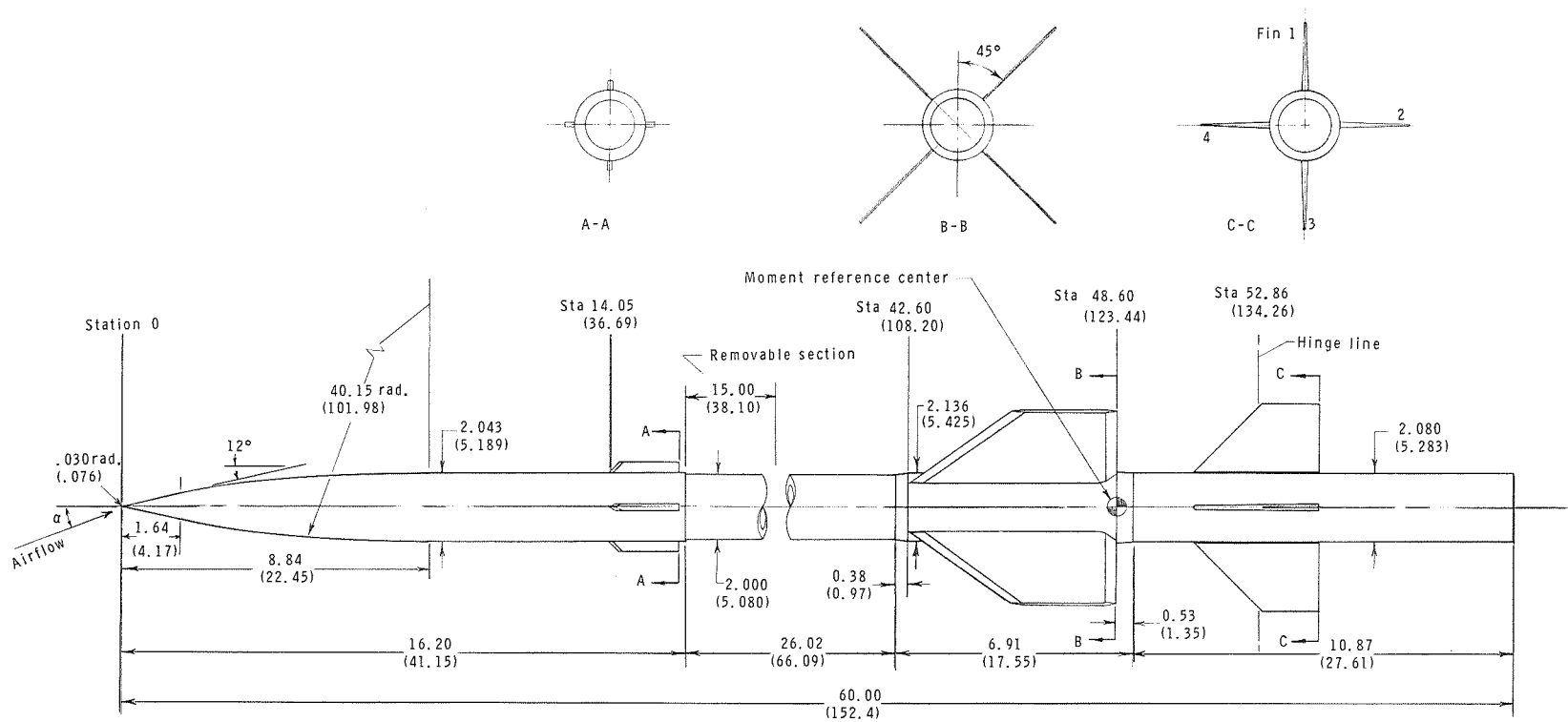
(b) Body

	Body
d, in. (cm)	2.043 (5.189)
S_{ref} , ft^2 (m^2)	0.0228 (0.00211)
S_{base} , ft^2 (m^2)	0.0236 (0.00219)
l (original body), in. (cm)	60.00 (152.40)
l (shortened body), in. (cm)	45.00 (114.30)

TABLE II.- FIN INCIDENCE ANGLES

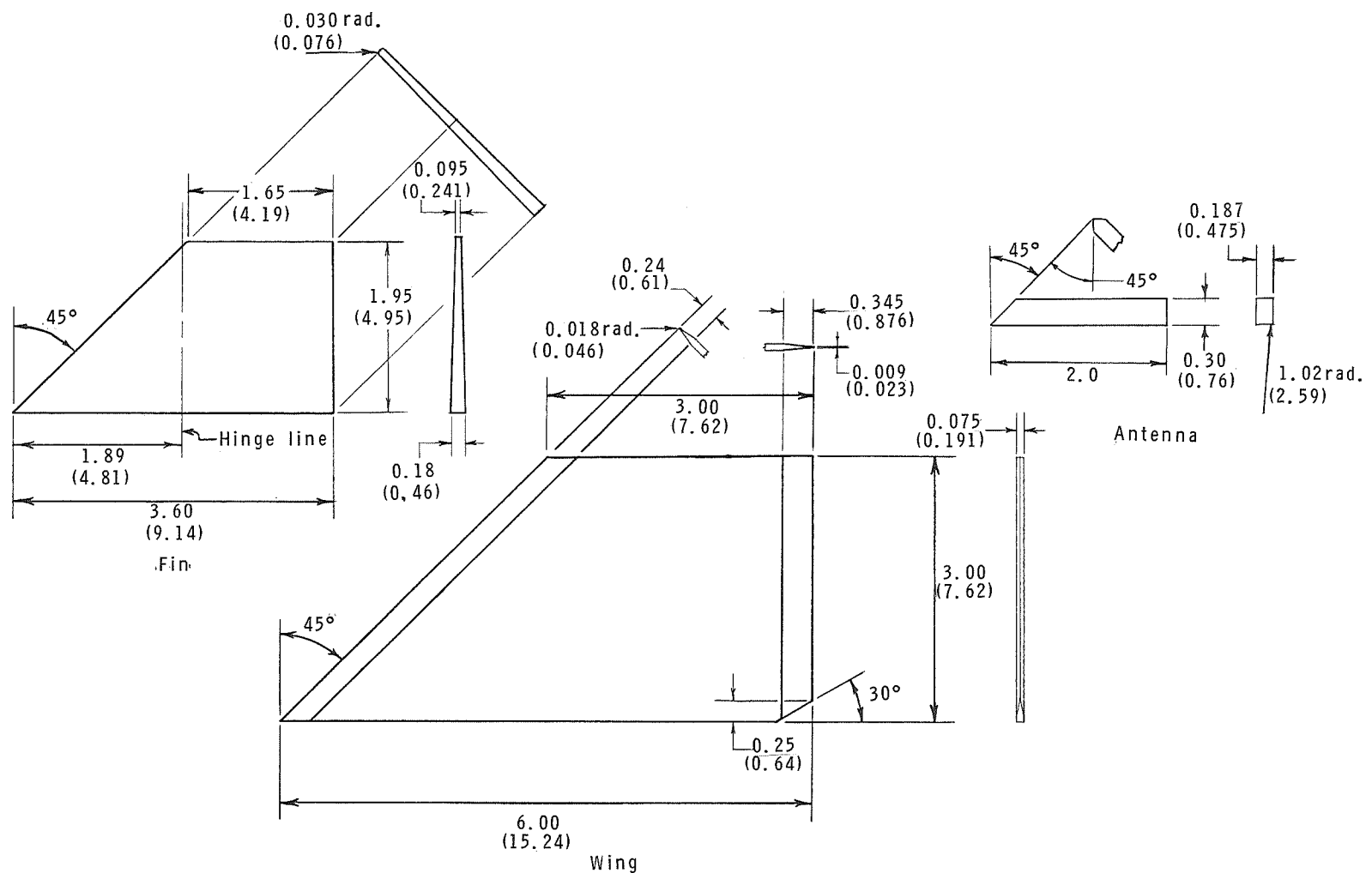
$[\delta_1$ and δ_3 are positive when the leading edge is to the right;
 δ_2 and δ_4 are positive when the leading edge is up]

Nominal deflection	δ_1 , deg	δ_2 , deg	δ_3 , deg	δ_4 , deg	Average δ_{pitch} , deg	Average δ_{roll} , deg	Average δ_{yaw} , deg
$\delta_{\text{pitch}}:$							
0	+0.6	-0.2	+0.6	+0.2	0	+0.1	+0.6
-3	+0.6	-3.2	+0.6	-4.5	-3.8	-0.3	+0.6
-6	+0.6	-5.3	+0.6	-6.4	-5.8	-0.3	+0.6
-12	+0.6	-12.0	+0.6	-12.9	-12.4	-0.2	+0.6
$\delta_{\text{roll}}:$							
-6	-6.9	+7.2	+6.1	-6.4	+0.4	-6.7	-0.4
-12	-13.1	+12.7	+11.9	-12.9	-0.1	-12.7	-0.6



(a) Complete model.

Figure 1.- Sketch of model. All linear dimensions are given in inches and parenthetically in centimeters.



(b) Details of appendages.

Figure 1.- Concluded.

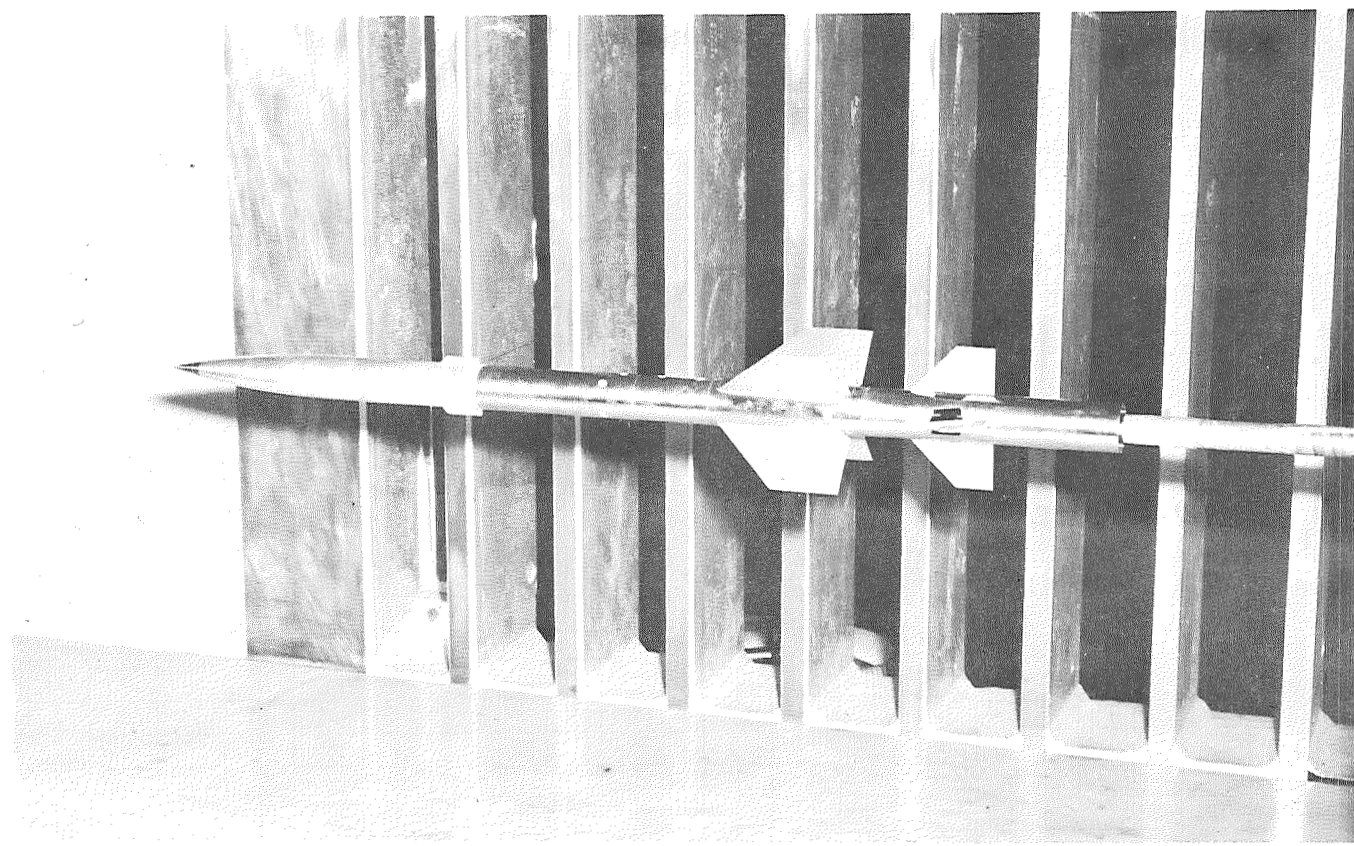


Figure 2.- Photograph of model. $l = 60$ m.

L-68-10204

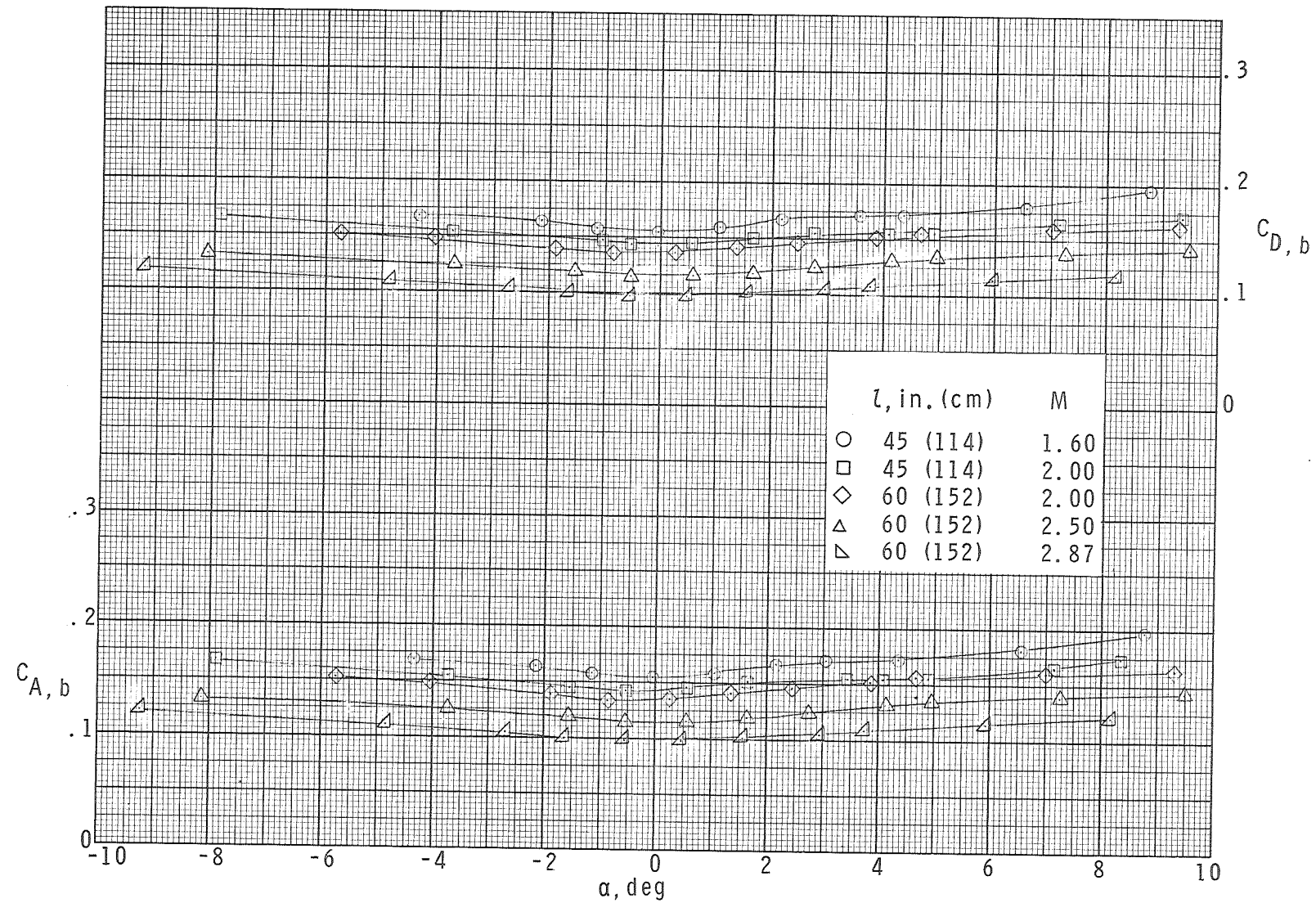
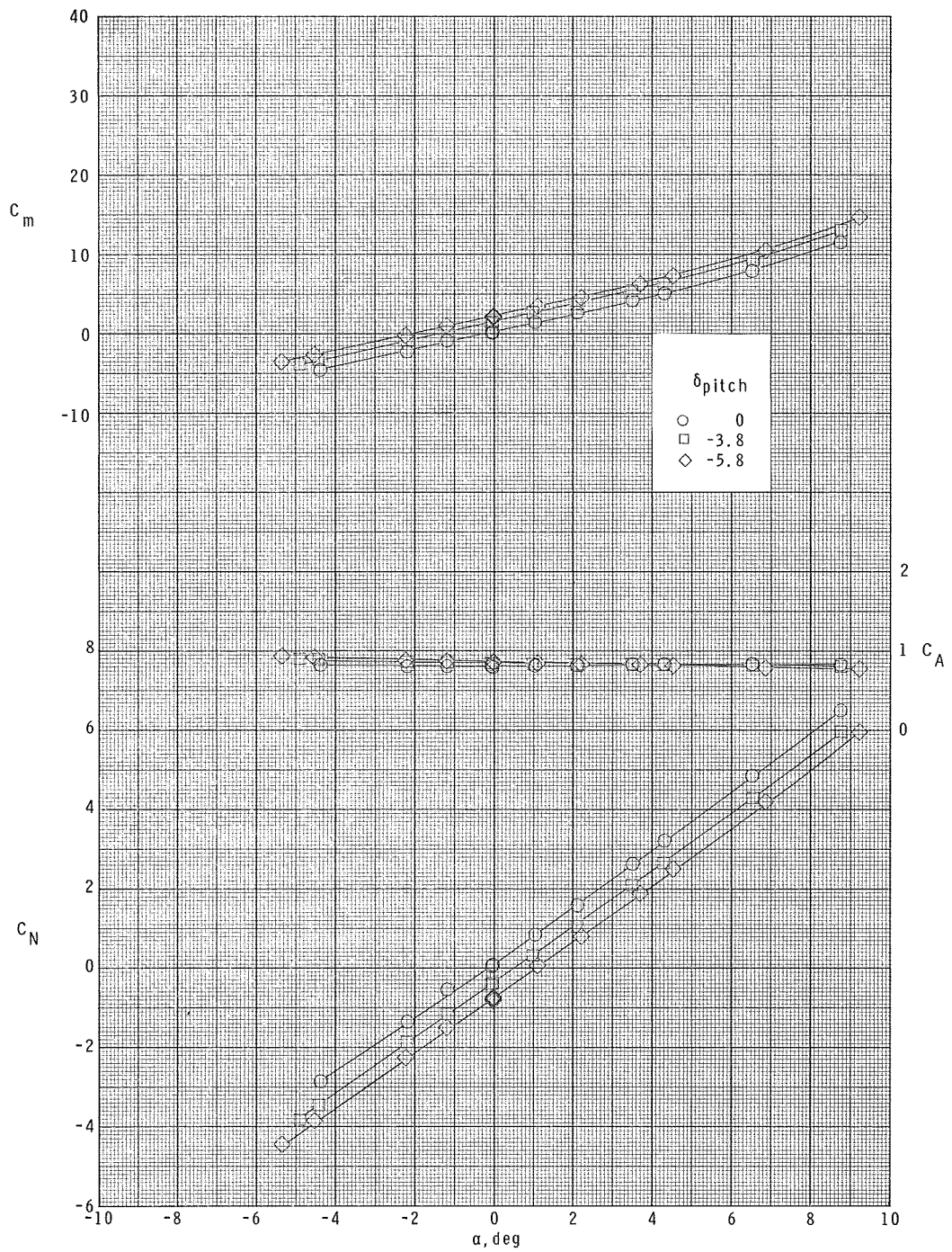
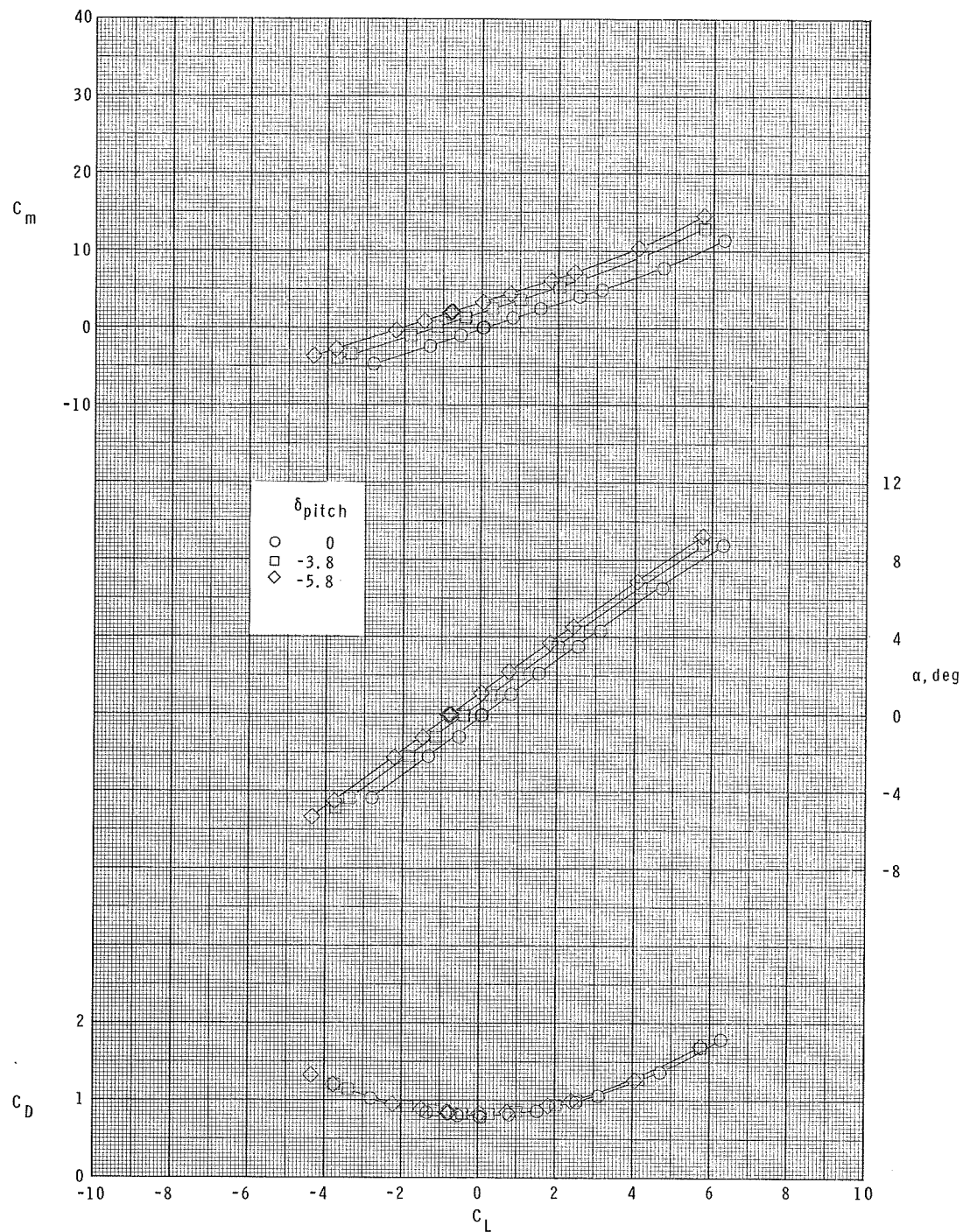


Figure 3.- Typical variation of base axial-force and drag coefficients with angle of attack. $\delta_{\text{pitch}} \approx 0 \approx \delta_{\text{roll}}$.



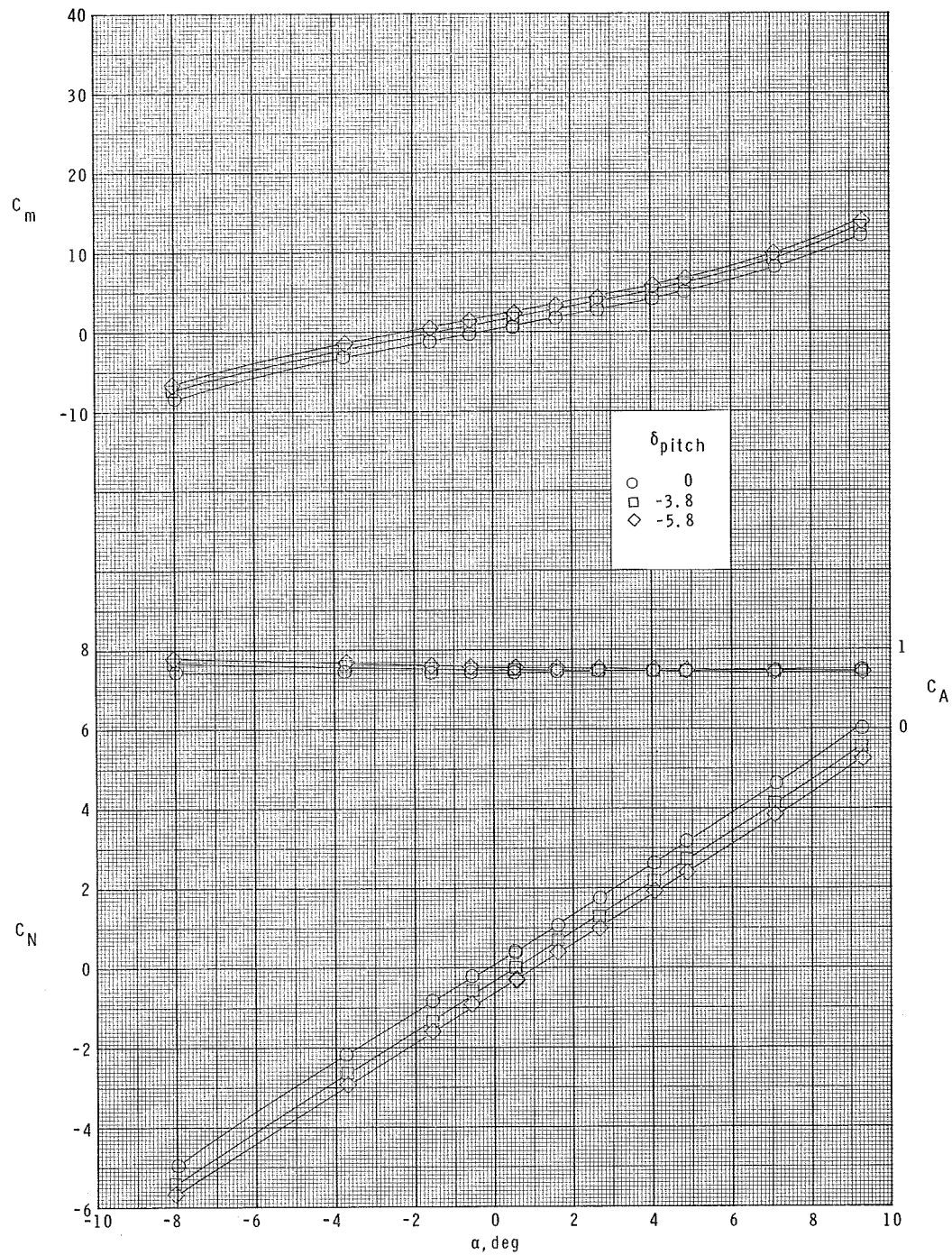
(a) $M = 1.60$; $l = 45$ in. (114 cm).

Figure 4.- Effect of fin deflection on longitudinal characteristics. Average values used for δ_{pitch} .



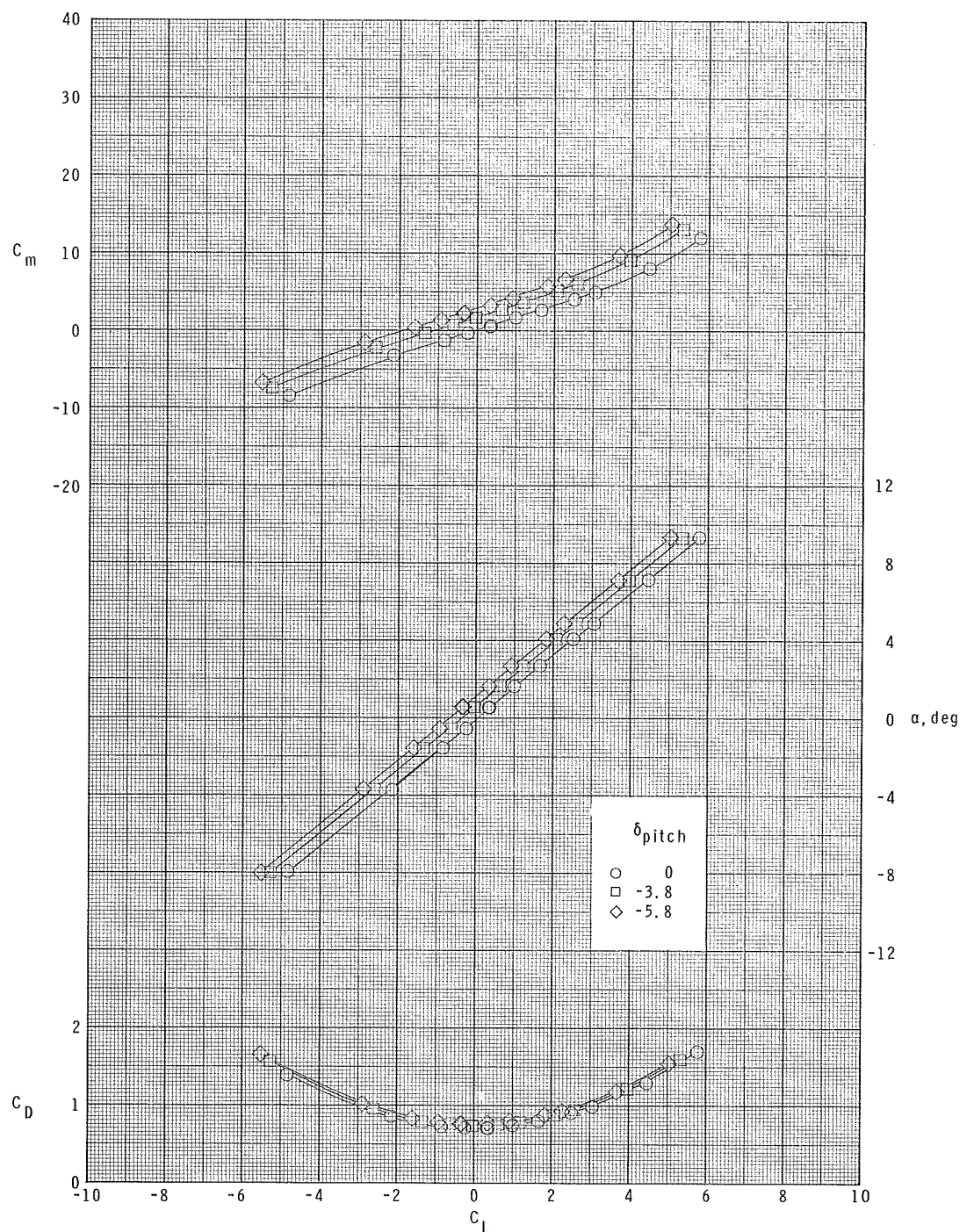
(a) Concluded.

Figure 4.- Continued.



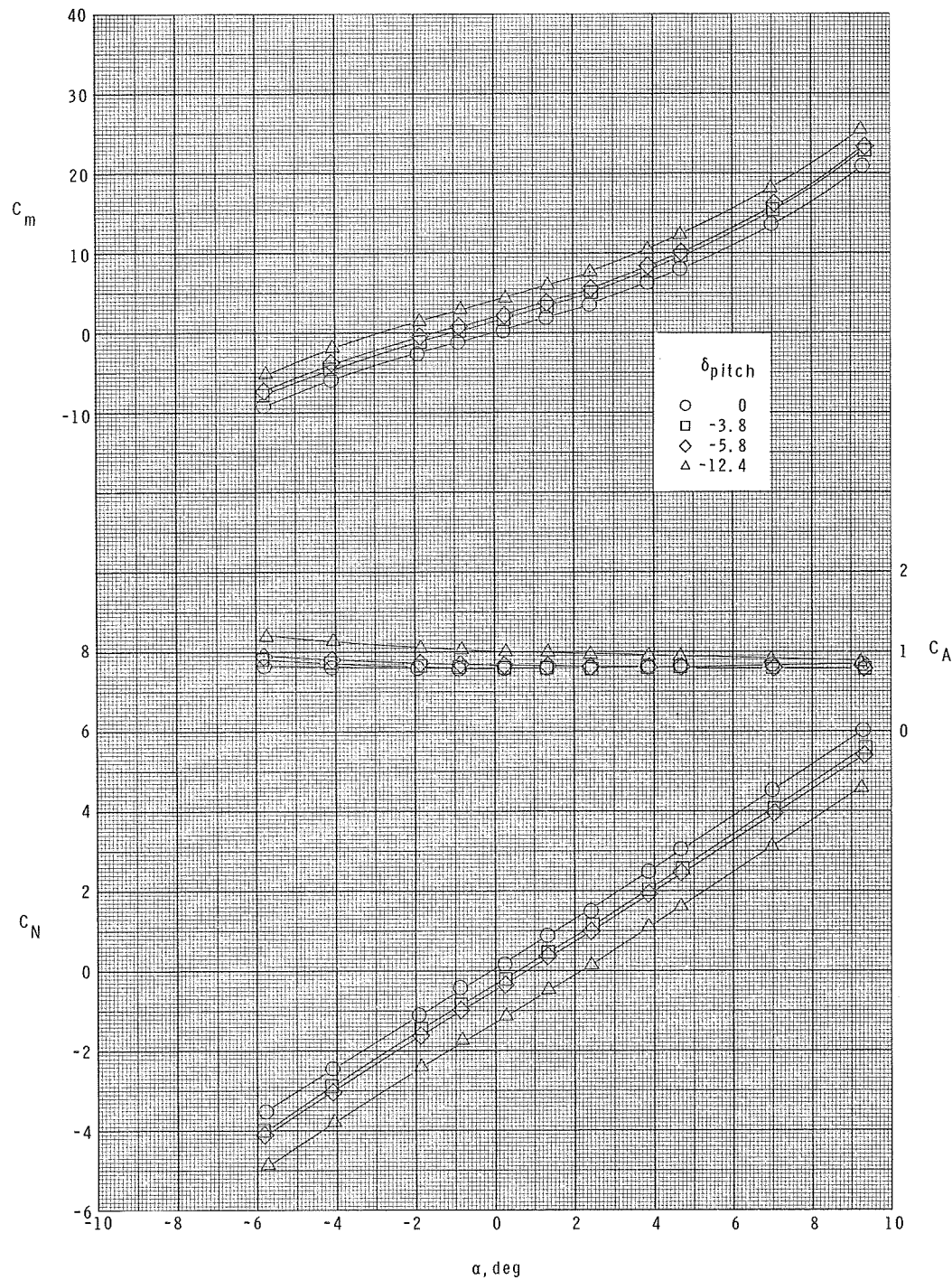
(b) $M = 2.00$; $l = 45$ in. (114 cm).

Figure 4.- Continued.



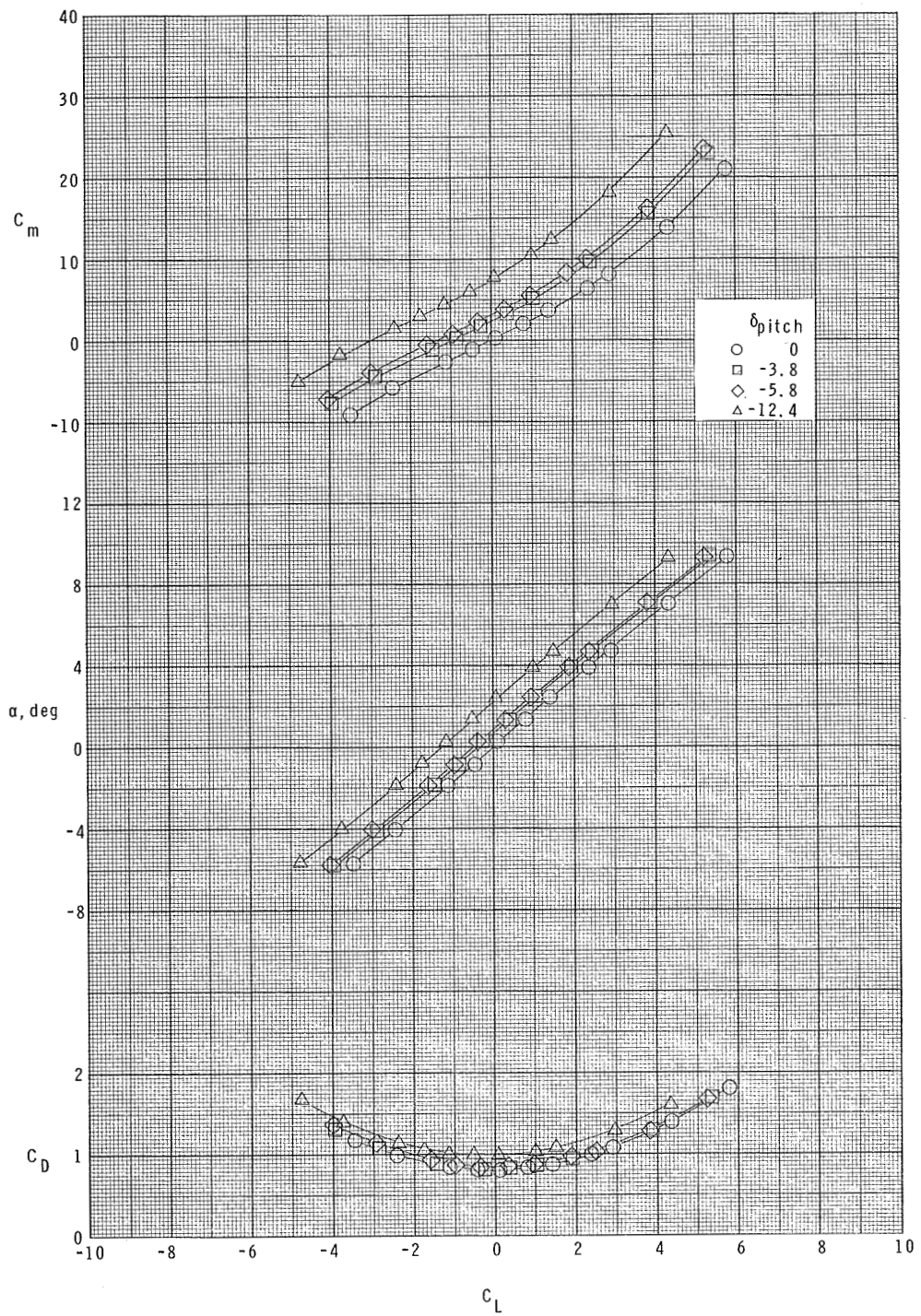
(b) Concluded.

Figure 4.- Continued.



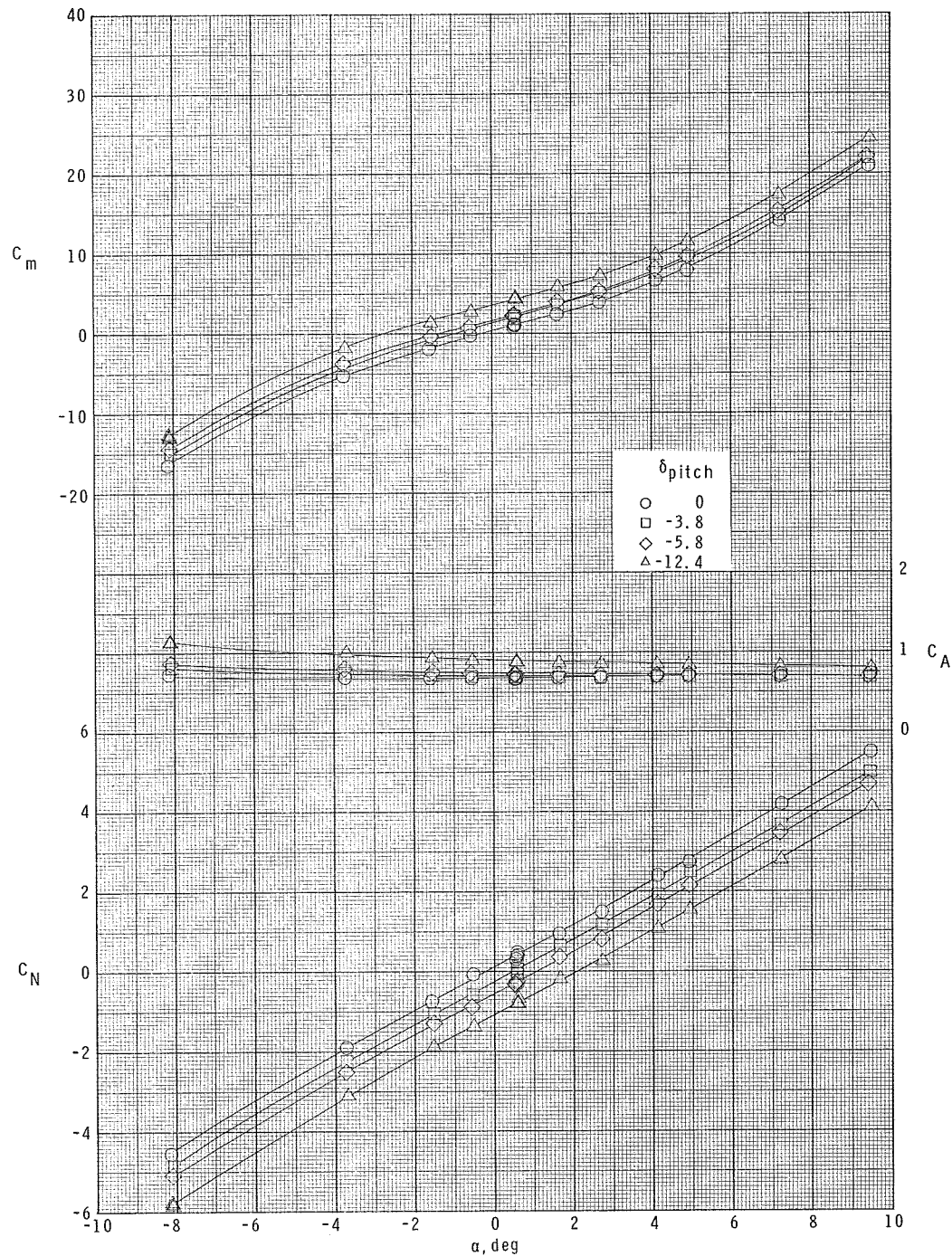
(c) $M = 2.00$; $l = 60$ in. (152 cm).

Figure 4.- Continued.



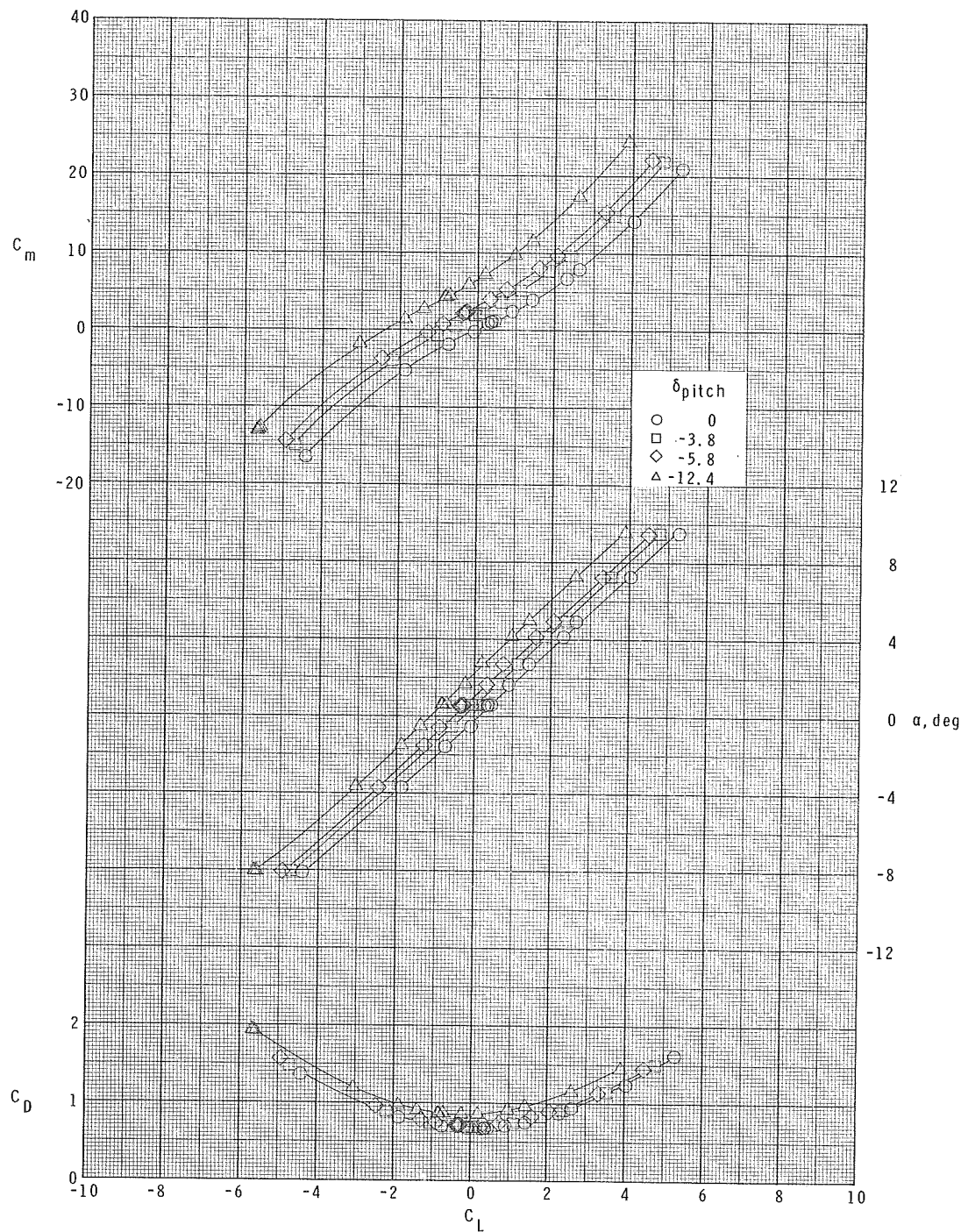
(c) Concluded.

Figure 4.- Continued.



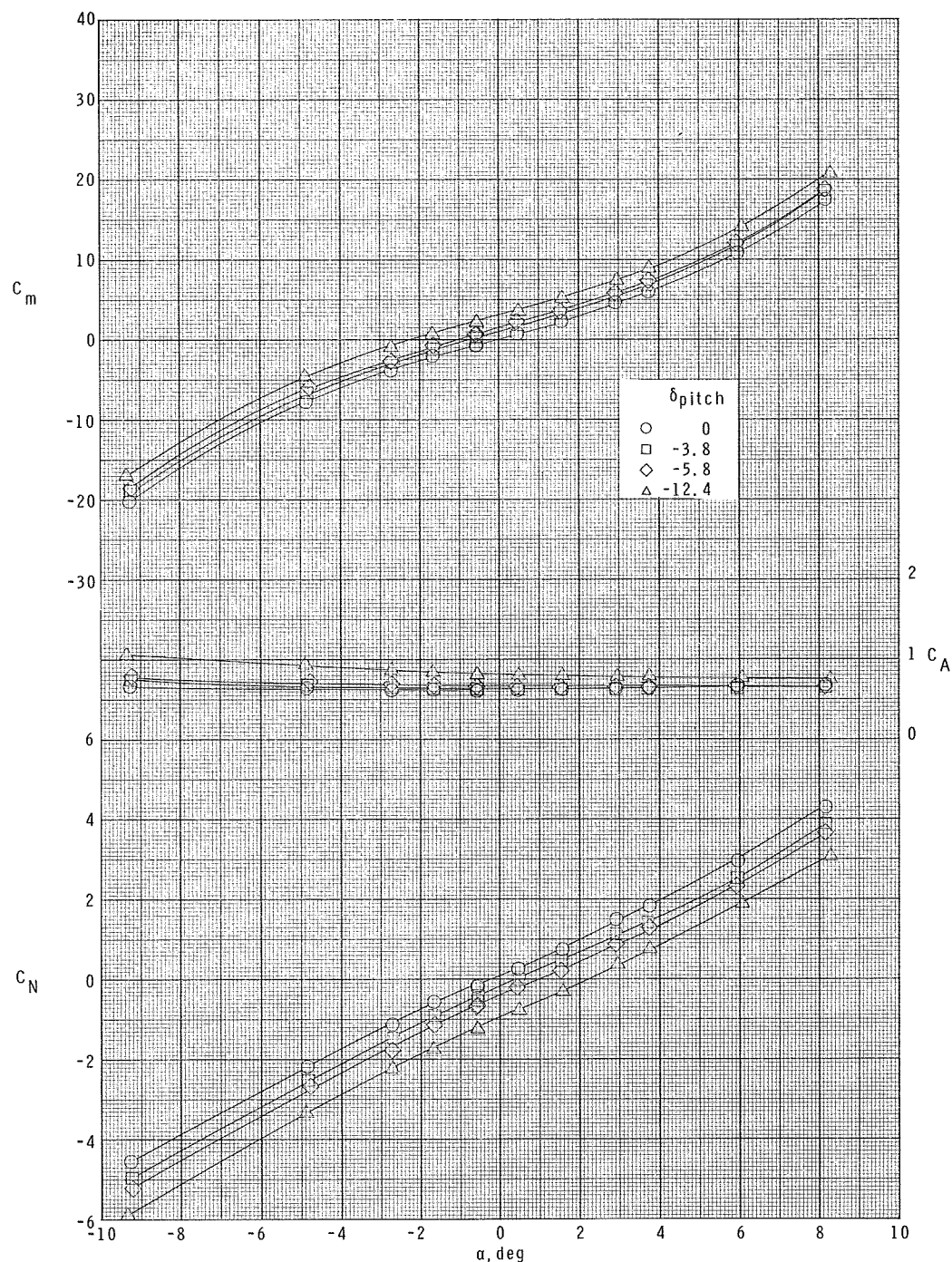
(d) $M = 2.50$; $l = 60$ in. (152 cm).

Figure 4.- Continued.



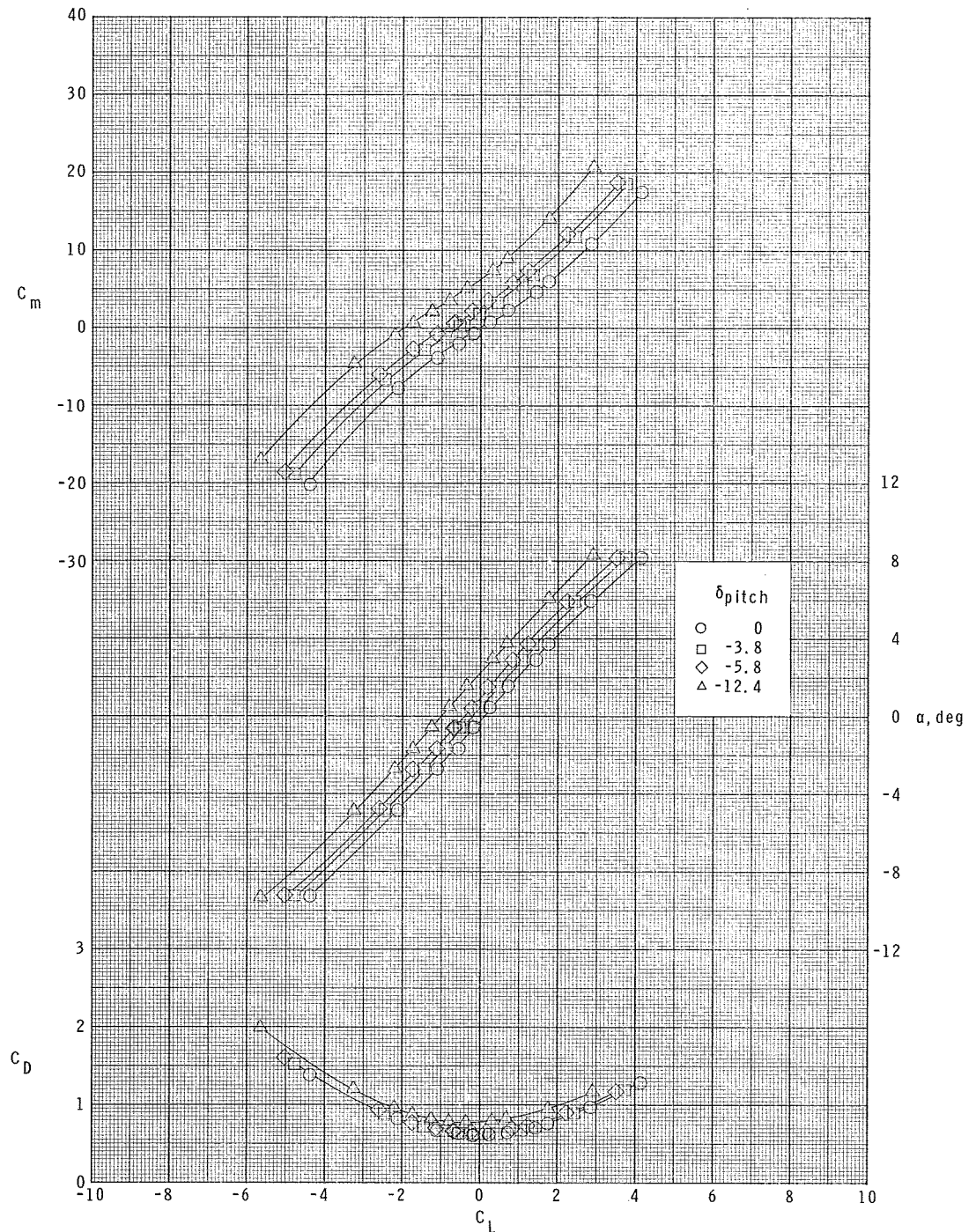
(d) Concluded.

Figure 4.- Continued.



(e) $M = 2.87$; $l = 60$ in. (152 cm).

Figure 4.- Continued.



(e) Concluded.

Figure 4.- Concluded.

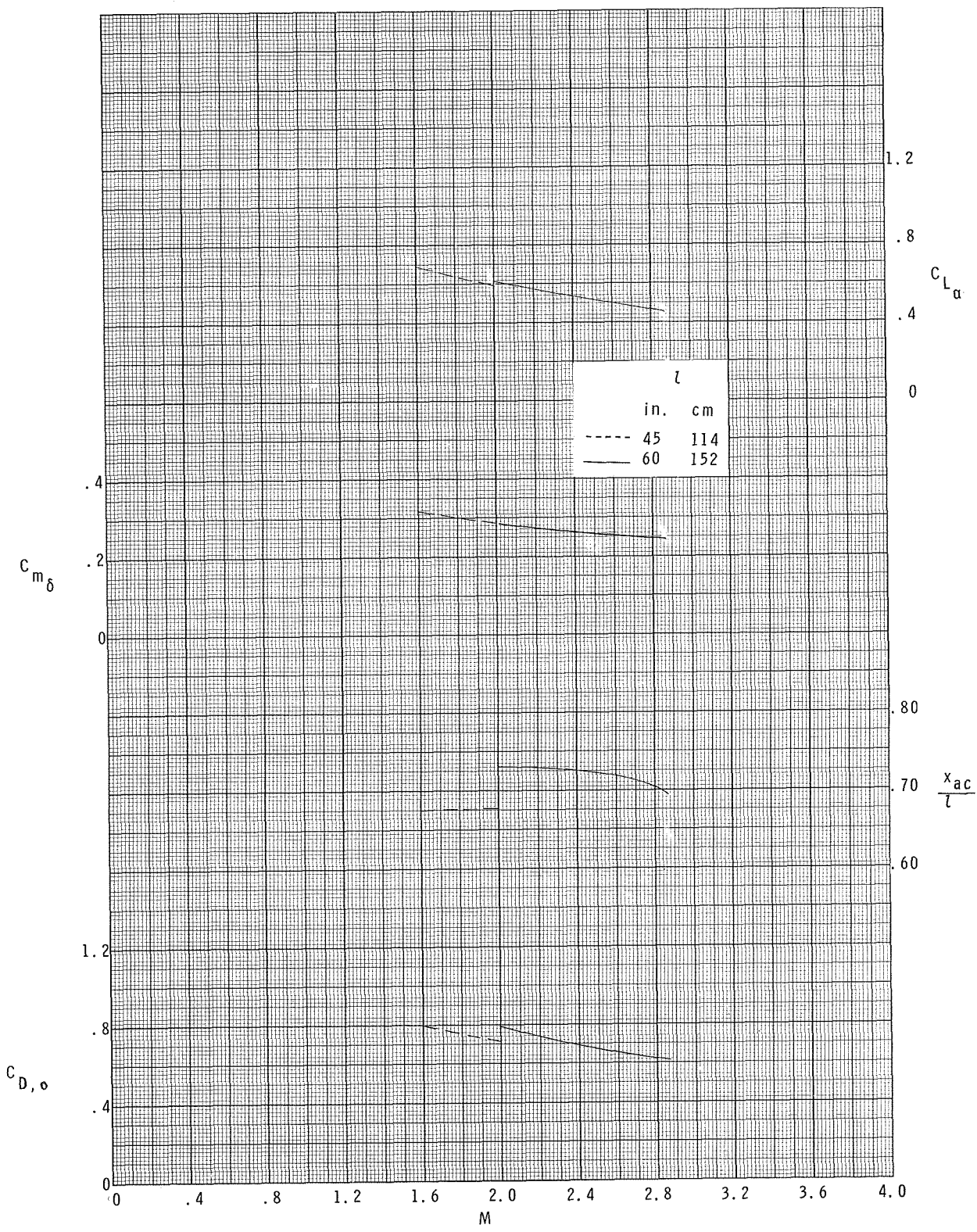
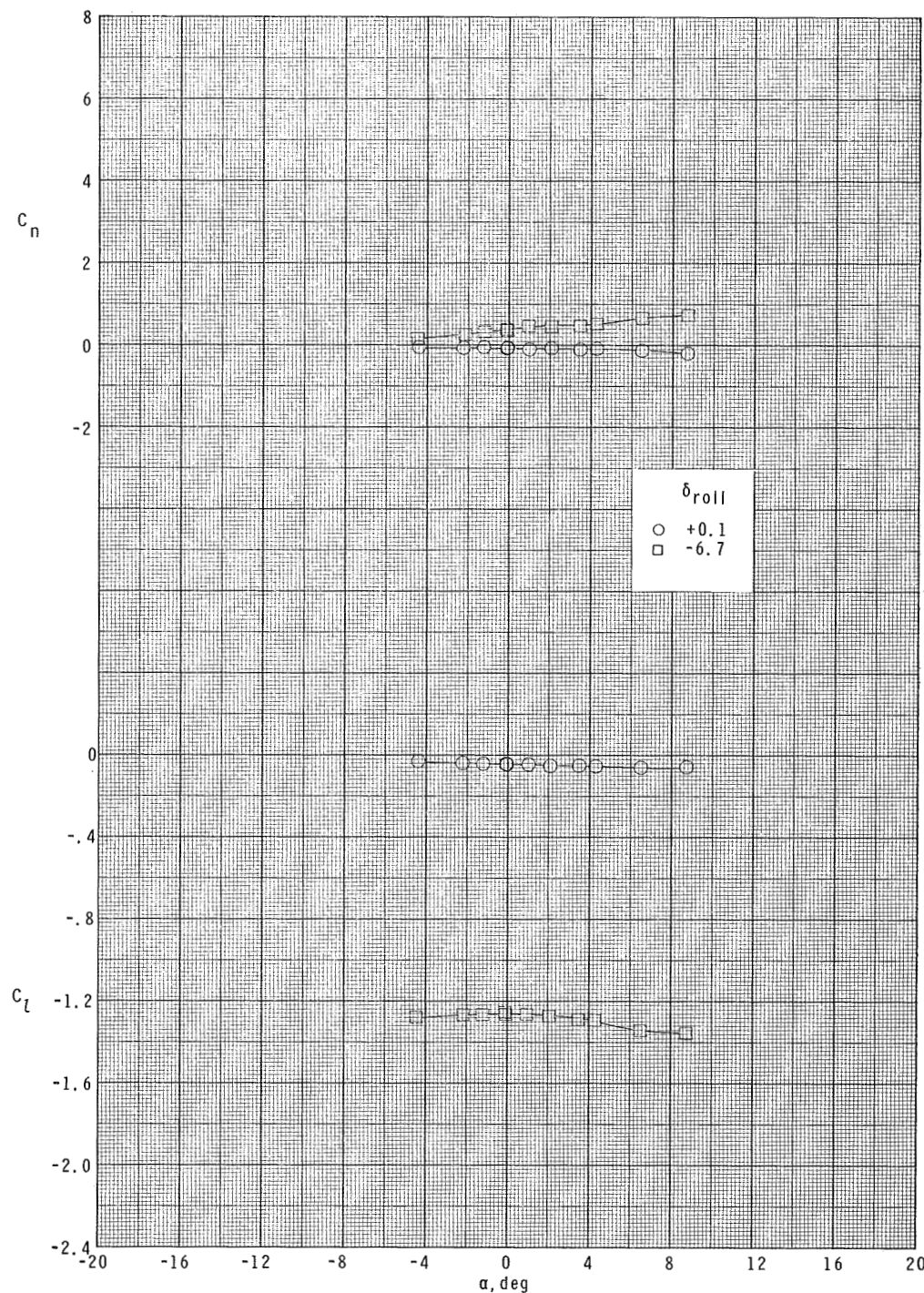
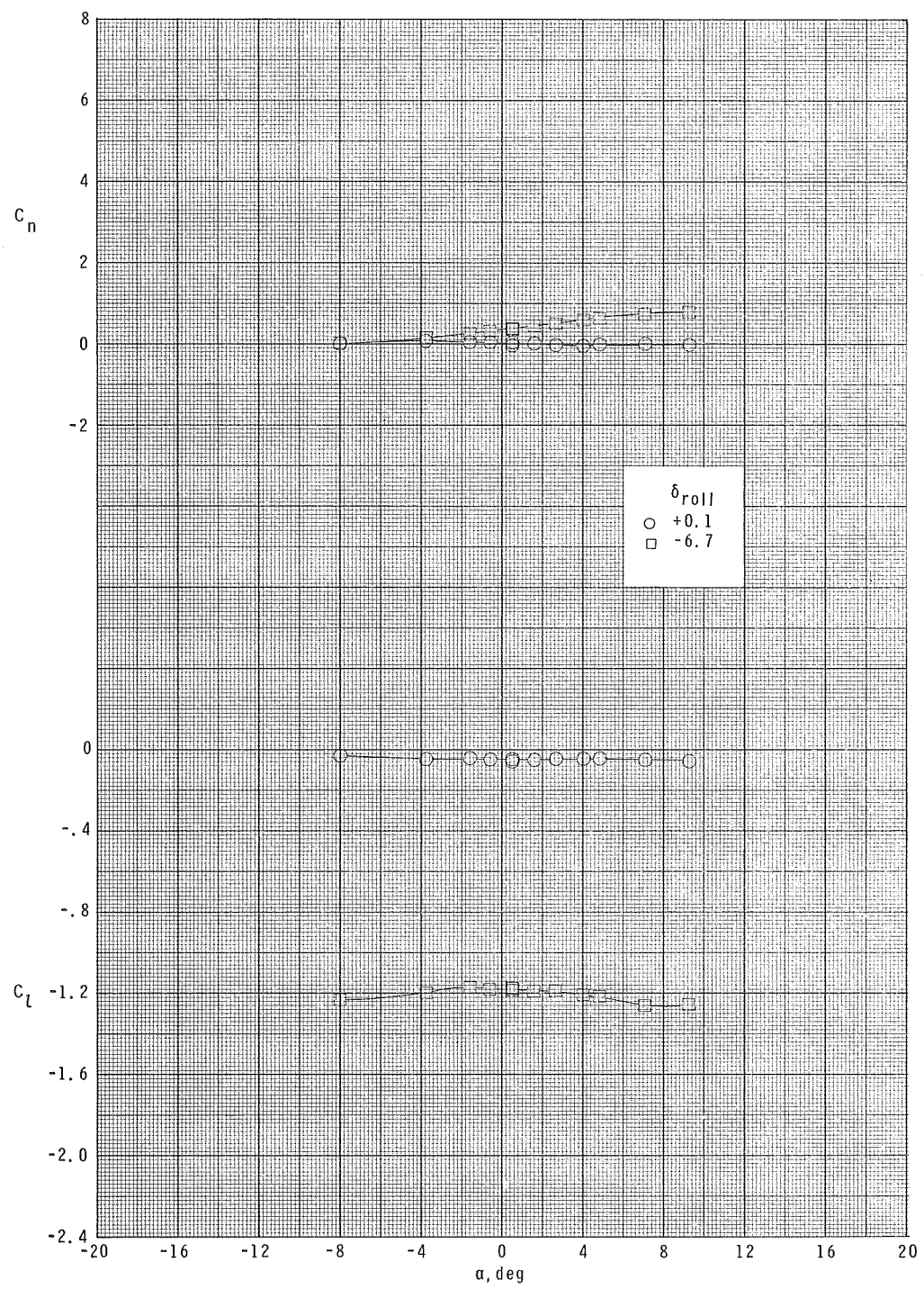


Figure 5.- Summary of the longitudinal aerodynamic characteristics.



(a) $M = 1.60$; $l = 45$ in. (114 cm).

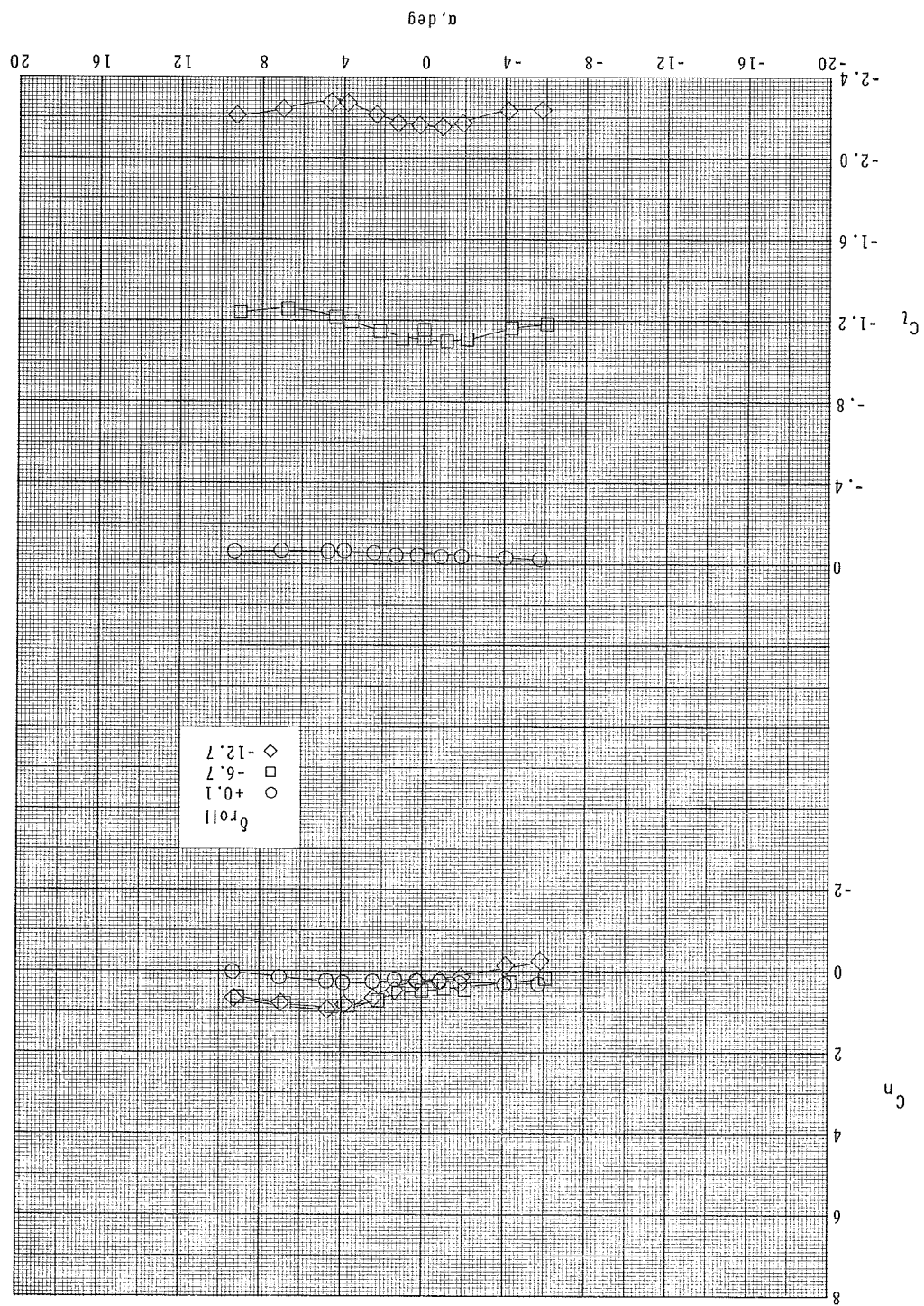
Figure 6.- Effect of fin deflection on roll-control characteristics. Average values used for δ_{roll} .

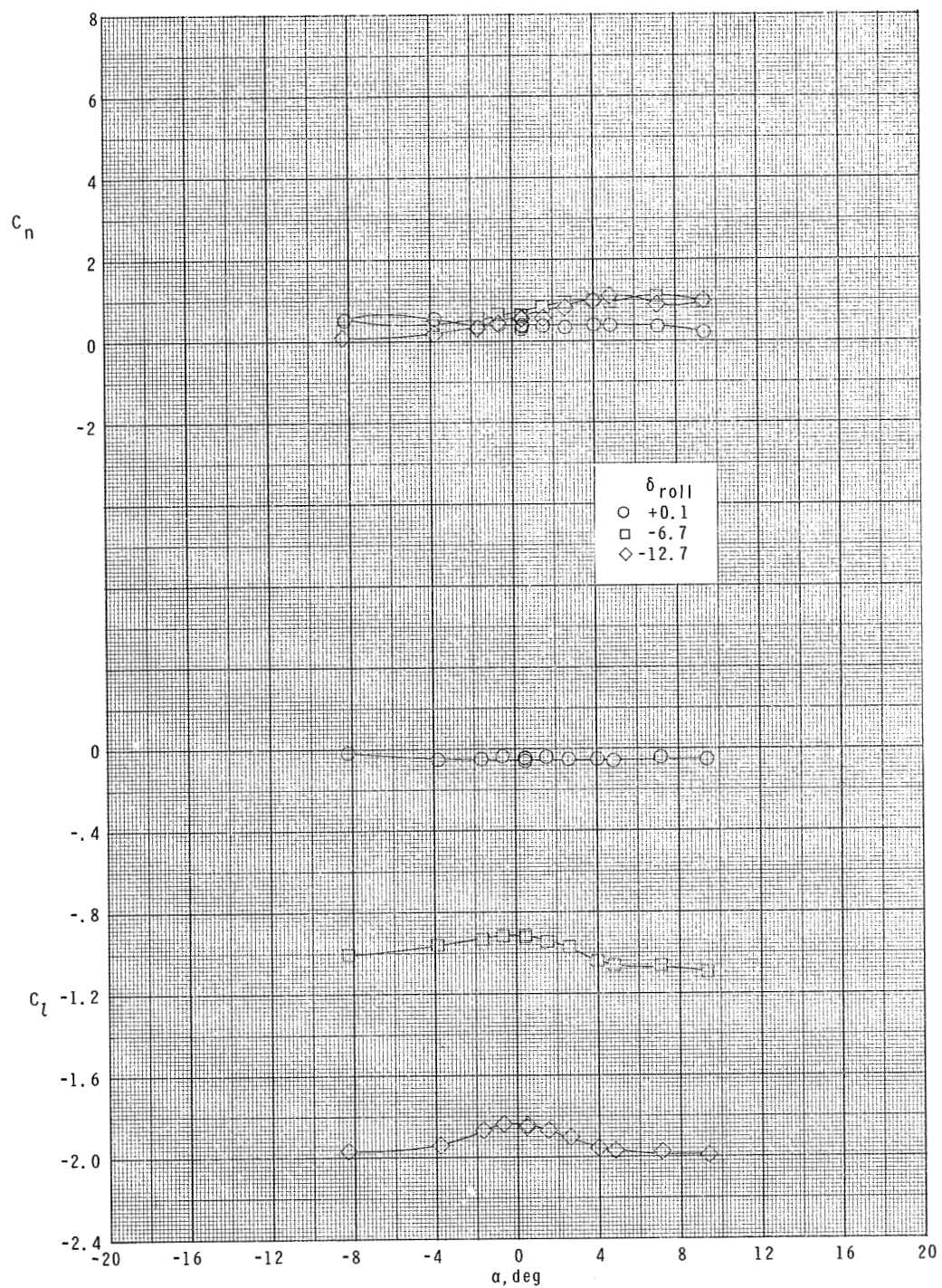


(b) $M = 2.00$; $l = 45$ in. (114 cm).

Figure 6.- Continued.

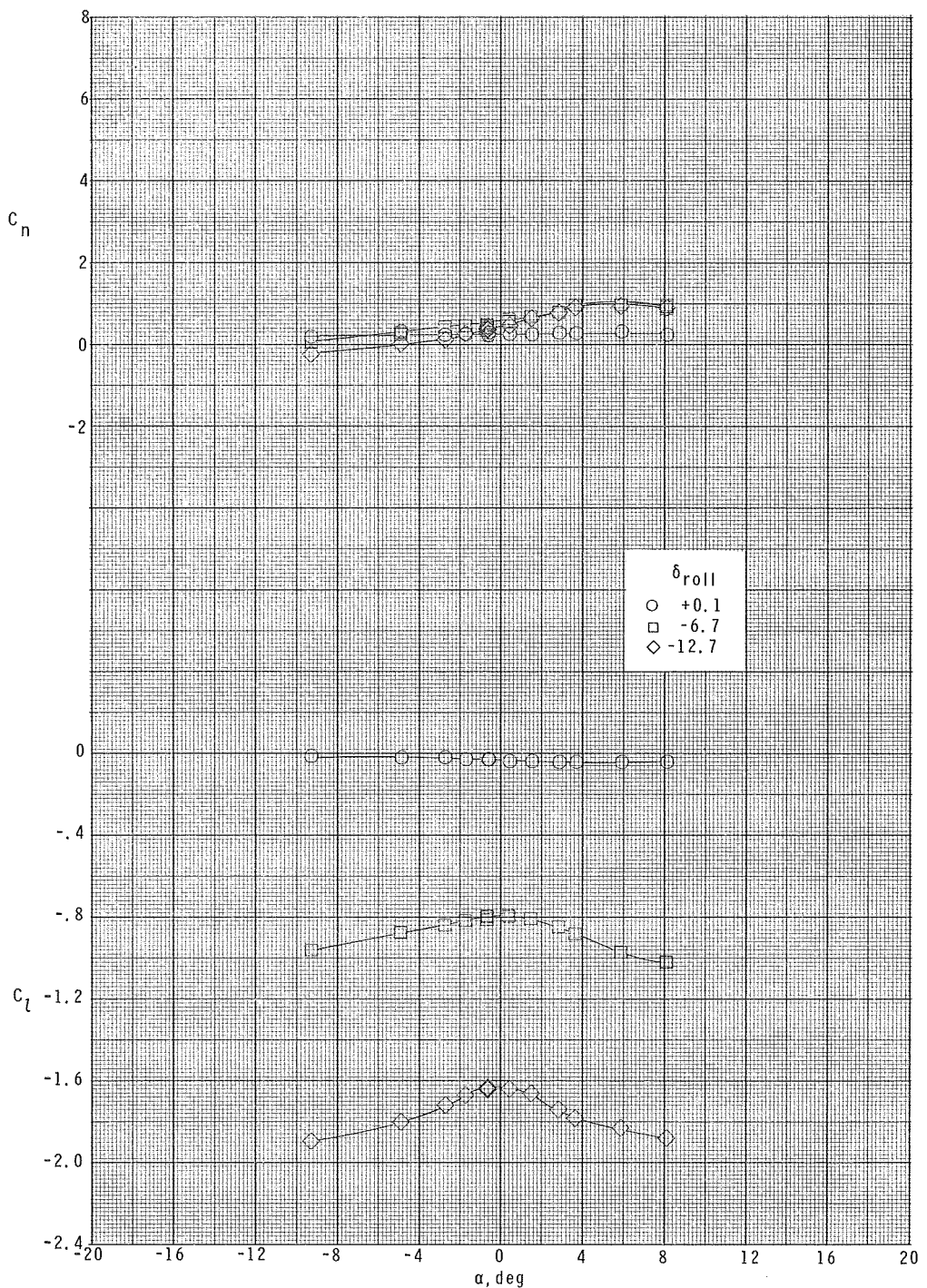
Figure 6.- Continued.

(c) $M = 2.00$, $l = 60$ in. (152 cm).



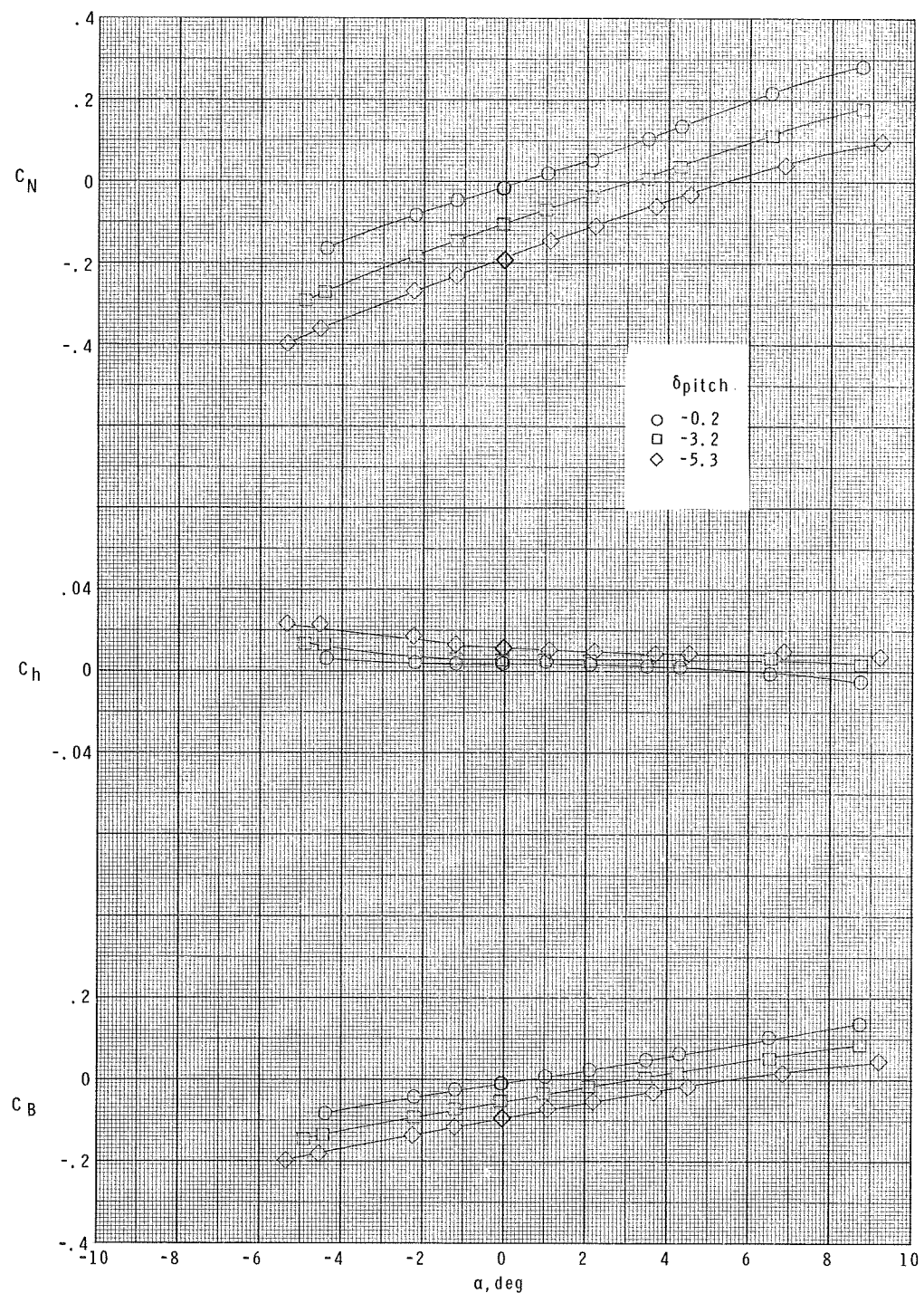
(d) $M = 2.50$; $l = 60$ in. (152 cm).

Figure 6.- Continued.



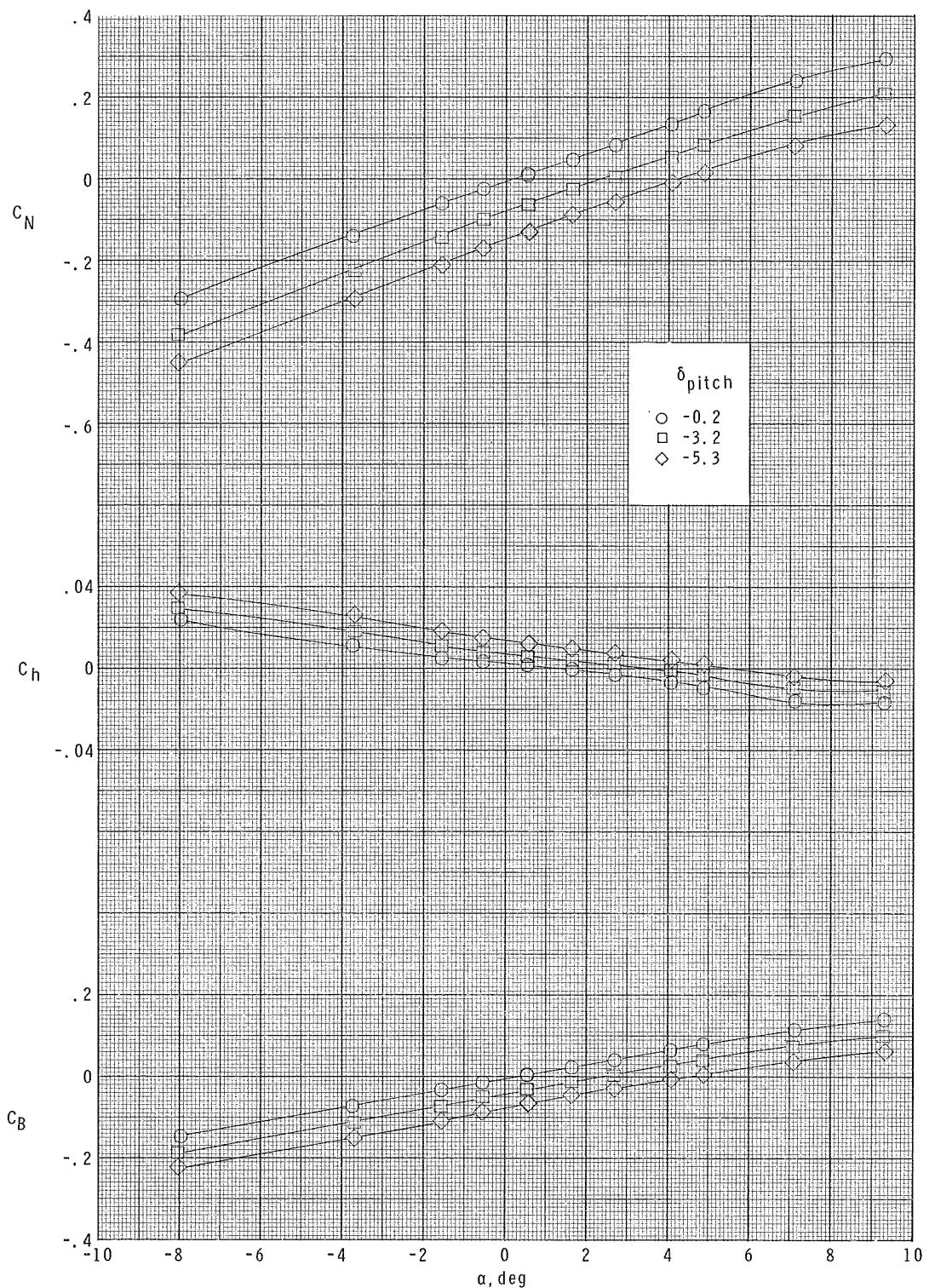
(e) $M = 2.87$; $l = 60$ in. (152 cm).

Figure 6.- Concluded.



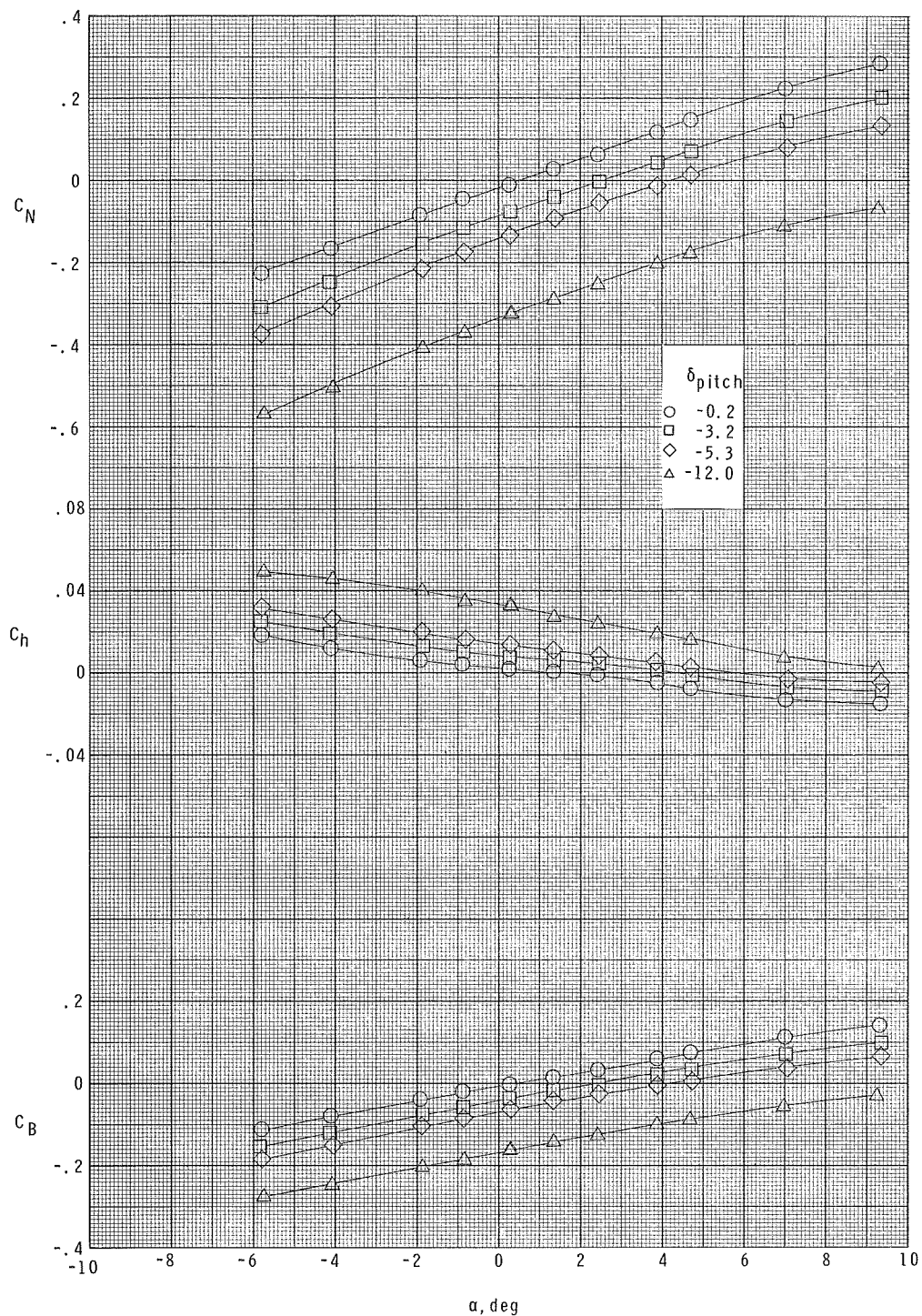
(a) $M = 1.60$; $l = 45$ in. (114 cm).

Figure 7.- Variation of fin load characteristics with angle of attack.



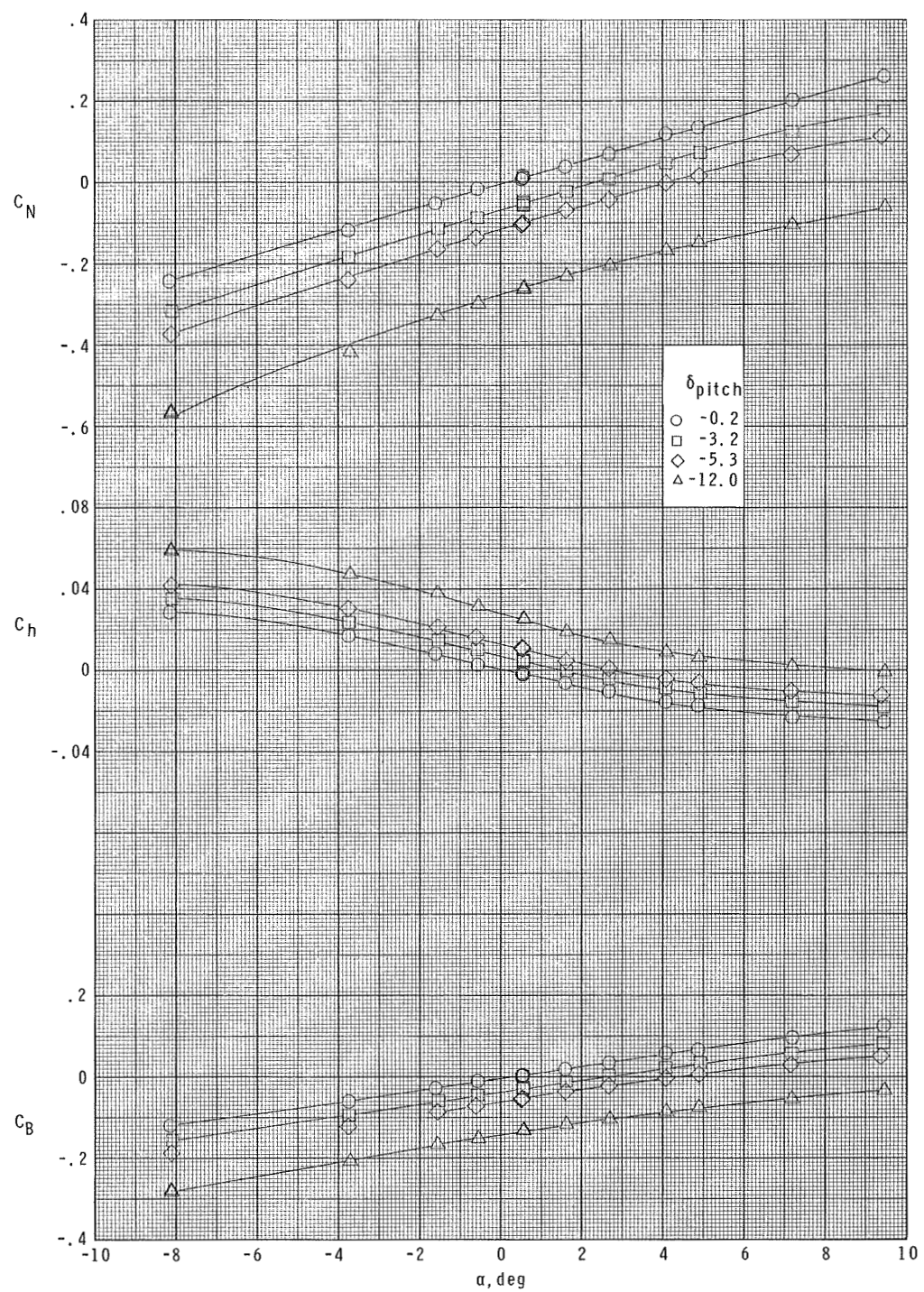
(b) $M = 2.00$; $l = 45$ in. (114 cm).

Figure 7.- Continued.



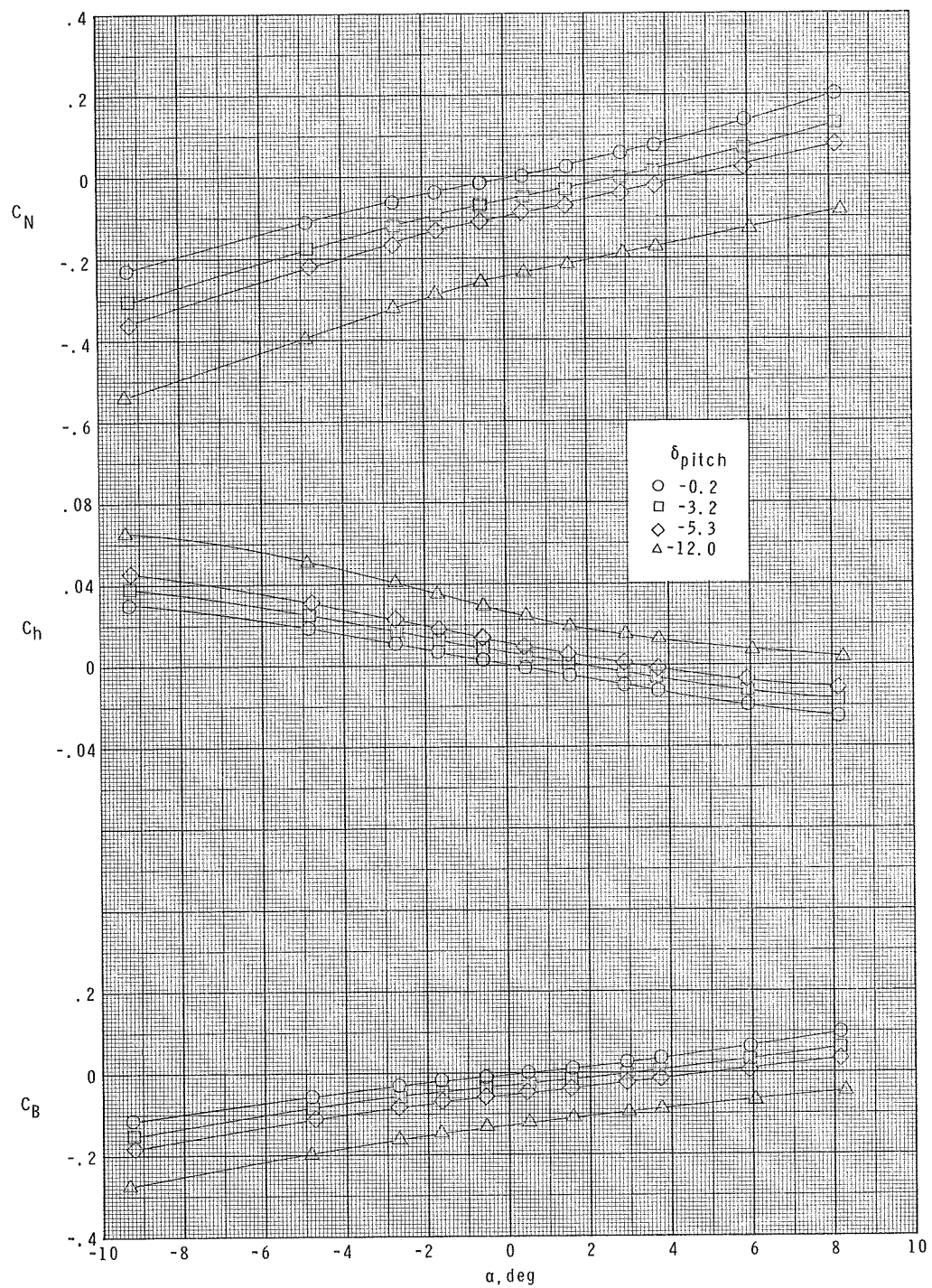
(c) $M = 2.00$; $l = 60$ in. (152 cm).

Figure 7.- Continued.



(d) $M = 2.50$; $l = 60$ in. (152 cm).

Figure 7.- Continued.



(e) $M = 2.87$; $l = 60$ in. (152 cm).

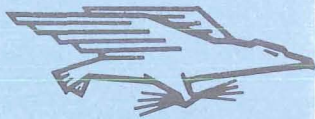
Figure 7.- Concluded.

NATIONAL AERONAUTICS AND SPACE ADMINISTRATION

WASHINGTON, D. C. 20546

OFFICIAL BUSINESS

FIRST CLASS MAIL



POSTAGE AND FEES PAID
NATIONAL AERONAUTICS AND
SPACE ADMINISTRATION

POSTMASTER: If Undeliverable (Section 158
Postal Manual) Do Not Return

"The aeronautical and space activities of the United States shall be conducted so as to contribute . . . to the expansion of human knowledge of phenomena in the atmosphere and space. The Administration shall provide for the widest practicable and appropriate dissemination of information concerning its activities and the results thereof."

— NATIONAL AERONAUTICS AND SPACE ACT OF 1958

NASA SCIENTIFIC AND TECHNICAL PUBLICATIONS

TECHNICAL REPORTS: Scientific and technical information considered important, complete, and a lasting contribution to existing knowledge.

TECHNICAL NOTES: Information less broad in scope but nevertheless of importance as a contribution to existing knowledge.

TECHNICAL MEMORANDUMS: Information receiving limited distribution because of preliminary data, security classification, or other reasons.

CONTRACTOR REPORTS: Scientific and technical information generated under a NASA contract or grant and considered an important contribution to existing knowledge.

TECHNICAL TRANSLATIONS: Information published in a foreign language considered to merit NASA distribution in English.

SPECIAL PUBLICATIONS: Information derived from or of value to NASA activities. Publications include conference proceedings, monographs, data compilations, handbooks, sourcebooks, and special bibliographies.

TECHNOLOGY UTILIZATION PUBLICATIONS: Information on technology used by NASA that may be of particular interest in commercial and other non-aerospace applications. Publications include Tech Briefs, Technology Utilization Reports and Notes, and Technology Surveys.

Details on the availability of these publications may be obtained from:

SCIENTIFIC AND TECHNICAL INFORMATION DIVISION
NATIONAL AERONAUTICS AND SPACE ADMINISTRATION
Washington, D.C. 20546